# BOUNDARY SHEAR STRESS DISTRIBUTION IN MEANDERING CHANNELS

*A thesis submitted to*

*National Institute of Technology, Rourkela*

*In partial fulfillment for the award of the degree*

*of*

**Master of Technology in Civil Engineering**

**With specialization in**

**Water Resources Engineering**


**By**

**Manaswinee Patnaik (211CE4253)**

**Under the supervision of**

**Professor K.C. Patra**




**Department of Civil Engineering**

**National Institute of Technology, Rourkela**

**Odisha-769008**


**May 2013**

**DEPARTMENT OF CIVIL ENGINEERING**
**NATIONAL INSTITUTE OF TECHNOLOGY, ROURKELA**

## DECLARATION

I hereby declare that this submission is my own work and that, to the best of my knowledge and belief, it contains no material previously published or written by another person nor material which to a substantial extent has been accepted for the award of any other degree or diploma of the university or other institute of higher learning, except where due acknowledgement has been made in the text.

**MANASWINEE PATNAIK**

**DEPARTMENT OF CIVIL ENGINEERING**
**NATIONAL INSTITUTE OF TECHNOLOGY, ROURKELA**

# CERTIFICATE

This is to certify that the thesis entitled **"Boundary Shear Stress Distribution in Meandering Channel"** is a bonafide record of authentic work carried out by **Manaswinee Patnaik** under my supervision and guidance for the partial fulfillment of the requirement for the award of the degree of Master of Technology in hydraulic and Water Resources Engineering in the department of Civil Engineering at the National Institute of Technology, Rourkela.

The results embodied in this thesis have not been submitted to any other University or Institute for the award of any degree or diploma.

**Date:**

**Place:** Rourkela

**Prof. K.C. Patra**
Department of Civil Engineering
National Institute of Technology, Rourkela
Rourkela-769008

## ACKNOWLEDGEMENTS

I am deeply indebted to **National Institute of Technology, Rourkela** for providing me the opportunity to pursue my Master's degree with all necessary facilities.

I would like to express my hearty and sincere gratitude to my project supervisor **Prof. K.C. Patra** whom sincere and affectionate supervision has helped me to carry out my project work. I would also like to thank **Prof. KK Khatua** for the support extended by him and his constant encouragement for the work has been the source of unparalleled enthusiasm for me.

I would like to record my gratitude to all faculty members of Water Resources Engineering who have constantly guided and inspired me till day in National Institute of Technology, Rourkela.

I am also thankful to staff members and students associated with the Fluid Mechanics and Hydraulics Laboratory of Civil Engineering Department, especially Mr. P. Rout for his useful assistance and cooperation during the entire course of the experimentation and helping me in all possible ways.

I wish to thank all of my fellow classmates for their kind help and co-operation extended during my course of study.

My parents have been my unfailing source of love and inspirations.

Date: MANASWINEE PATNAIK

# ABSTRACT

Precise estimation of boundary shear force distribution is essential to deal with various hydraulic problems such as channel design, channel migration and interaction losses. Bed shear forces are useful for the study of bed load transfer where as wall shear forces presents a general view of channel migration pattern. Meander formation in rivers is an intricate phenomenon that results from erosion on outer bank and deposition on the inner side. So the analysis of meandering channels under different geometric and hydraulic condition are necessary to understand one of the flow properties such as distribution of boundary shear which is a better indicator of secondary flows than velocity, on different parameters like aspect ratio, sinuosity, ratio of minimum radius of curvature to width and hydraulic parameter such as relative depth.

With the purpose of obtaining shear stress distribution at the walls and on the bed of compound meandering channel, experimental data collected from laboratory under different discharge and relative depths maintaining the geometry, slope and sinuosity of the channel constant, are analyzed and confronted. Preston-tube technique is used to collect velocity heads at various intervals along the wetted perimeter and within the flow that helps to calculate shear stress values using calibration curves proposed by Patel (1965). The distributions of boundary shear stress along the channel wetted perimeter are plotted for both in bank and overbank flow conditions. Based on experimental results, the effect of aspect ratio and sinuosity on wall (inner and outer) and bed shear forces are evaluated in meandering wide channels ($B/H > 5$) and having a sinuosity of 2.04. Equations are developed to determine the percentage of wall and bed shear forces in smooth trapezoidal channel for in bank flows only. The proposed equations are compared with previous studies and the model is extended to wide channels. A quasi1D model Conveyance Estimation System (CES) were then applied in turn to the same compound

meandering channel to validate with the experimental shear velocity which ultimately relates to the boundary shear stress. It has been found that the CES results underestimate the shear velocity.

A3D modelling software ANSYS-CFX 13.0 is employed to derive the contours of longitudinal, lateral and resultant bed shear stress, for a 60 degree meandering channel using Large Eddy Scale (LES) model.

**Key Words:**

*Aspect ratio; Boundary shear; Compound channel; Conveyance; In-bank flow; Interaction loss; Meander; Over-bank flow; Preston-tube; Relative depth; Sinuosity*

## TABLE OF CONTENTS

## LIST OF TABLES

## LIST OF FIGURES AND PHOTOGRAPHS

## LIST OF SYMBOLS

| | |
|---|---|
| $B$ | width of the channel; |
| $C_r$ | Courant number; |
| $C_s$ | Smagorinsky constant; |
| $d$ | outside diameter of the probe; |
| $g$ | acceleration due to gravity; |
| $G$ | Gaussian filters; |
| $H$ | in bank depth of flow; |
| $H'$ | over bank depth of flow; |
| $h$ | main channel bank full depth; |
| $k$ | turbulent kinetic energy; |
| l | length scale of unresolved motion; |
| $P$ | wetted perimeter; |
| $Q$ | discharge; |
| $R$ | hydraulic radius; |
| $S_r$ | Sinuosity; |
| $S_{ij}$ | Resolved strain rate tensor; |
| $S$ | bed slope of the channel; |
| $y$ | lateral distance along the channel bed; |
| $z$ | vertical distance from the channel bed; |
| $\alpha$ | aspect ratio; |
| $\rho$ | Fluid density; |

$\theta$ angle between channel bed and horizontal;

$v$ kinematic viscosity;

$\varepsilon$ turbulent kinetic energy dissipation rate;

$\omega$ specific dissipation;

$\sigma_{ij}$ normal stress component on plane normal to i along j;

$\tau_{ij}$ shear stress component on plane normal to i along j;

$\bar{u}_i'$, $\bar{u}_j'$ time averaged instantaneous velocity component along i,j directions

$\tau_0$ overall boundary shear stress;

$\mu$ coefficient of dynamic viscosity;

$x^*$ logarithmic of the dimensionless pressure difference;

$y^*$ logarithmic of the dimensionless shear stress;

$\Delta P$ Preston tube differential pressure;

$\Delta h$ difference between dynamic and static head;

$(\%SF)_w$ percentage shear force at walls;

$(\% SF)_b$ percentage shears force on bed;

$(\% SF_{w)mod}$ modeled percentage shear force at walls;

$(\% SF_{w)act}$ observed percentage shear force at walls

**Subscripts**

| | |
|---|---|
| *a/act.* | actual |
| *b, bed* | bed |
| *h* | hydraulic |
| *r* | relative |
| *t* | theoretical |
| T | total |
| *w* | wall |
| *mod.* | modelled |
| *i, j, k* | *x, y, z* directions respectively |
| *i, inner* | inner bank or wall of meandering channel |
| *o, outer* | outer bank or wall of meandering channel |

# INTRODUCTION

## 1.1 RIVER AND FLOODING

River and river valleys have been very crucial in the development of civilization. River has always been main source of water for agriculture, domestic needs, industries etc. Also river provide as with energy, recreation and transportation routes. Eventually, it becomes hard to believe that during flood a gentle river inundate its flood plain thereby causing serious damage to the lives and shelter of the people residing in low-lying areas. Nowadays debate on flooding is gaining momentum due to combining consequences of climate change. From recent times, river engineer's devise solutions by designing flood defenses so as to ensure minimum damage from flooding. Generally river engineer's use hydraulic model to make flood prediction. The hydraulic model incorporates many flow features such as accurate discharge, average velocity, water level profile and shear stress forecast. Prior to producing hydraulic models capable of modeling all these flow features detailed knowledge on open channel hydrodynamics is required. In this regard, first comes the understanding of geometrical and hydraulic parameters of the river streams. Even the flow properties in rivers vary with the geometrical shape.

Broadly streams are classified as straight, braided and meandering. Almost all natural rivers meander. Natural rivers are seldom straight except for short distances. Inglis (1947) was probably the first to define meandering and it states "where however, banks are not tough enough to withstand the excess turbulent energy developed during floods, the banks erode and the river widens and shoals". Otherwise stated, meandering channels are the channel that winds its way across the floodplain. The flow path in a meandering channel continuously changes along its course. Due to this the energy dissipation is not uniform over the meander length. The motion in

meandering channels comprised of two components, the longitudinal component in stream wise direction which is nearly uniform and gradually varied and transverse component varies significantly over a meander wavelength. In general, a meander is a bend in a sinuous water course which is formed when flowing water in a stream erodes the outer bank and widens its valley. Theoretically a sine generated curve well represents a meander channel. The sinuosity or meander index which quantifies how much a river course deviates from the shortest possible path is one of the criterions which control the velocity and shear distribution in meandering channel.

## 1.2 BOUNDARY SHEAR DISTRIBUTION

When water flows in a channel the force developed in the flow direction is resisted by reaction from channel bed and side walls. This resistive force is manifested in the form of boundary shear force. Otherwise stated, tractive force, or boundary shear stress, is the tangential component of the hydrodynamic forces acting along the channel bed. Distribution of boundary shear force along the wetted perimeter directly affects the flow structure in an open channel. Knowledge on boundary shear stress distribution is necessary to define velocity profile and fluid field. Also computation of bed form resistance, sediment transport, side wall correction, cavitations, channel migration, conveyance estimation, and dispersion are among the hydraulic problems which can be solved by bearing the idea of boundary shear stress distribution.

From theoretical considerations, in steady uniform flow the tractive force is related to channel bed slope, hydraulic radius and unit weight of fluid. However it is established that such forces even in straight prismatic channel with simple cross-sectional geometry are not uniform. Moreover the tractive force is a turbulent quantity composed of a fluctuating component

superimposed on the mean value. The non-uniformity in shear stress is mostly due to this fluctuating component which is interpreted as secondary currents and is generated by the anisotropy between the vertical and transverse turbulent intensities, this is given by Gessner, 1973. Although secondary velocity comprises only 2-3% of primary mean velocity it convects momentum, vorticity and energy towards the corners and subsequently transports them away along the boundary walls. Tominaga *et al.* (1989) and Knight and Demetriou (1983) showed that boundary shear stress increases where secondary currents flow towards the wall and shear stress decreases as they flow away from the wall. The presence of secondary flow cells in main flow influences the distribution of shear stress along the channel wetted perimeter which is illustrated in Fig. 1.1. Other factors that affect the distribution of shear stress in straight channel are shape of the cross-section, number and structure of secondary flow cells, depth of flow, sediment concentration and the lateral-longitudinal distribution of wall roughness. In meandering channels the factors increases by many folds due to accretion in 3-Dimensional nature of flow. Sinuosity of the meandering channel is considered to be a critical parameter for calculating the percentage of shear force at channel walls and bed.

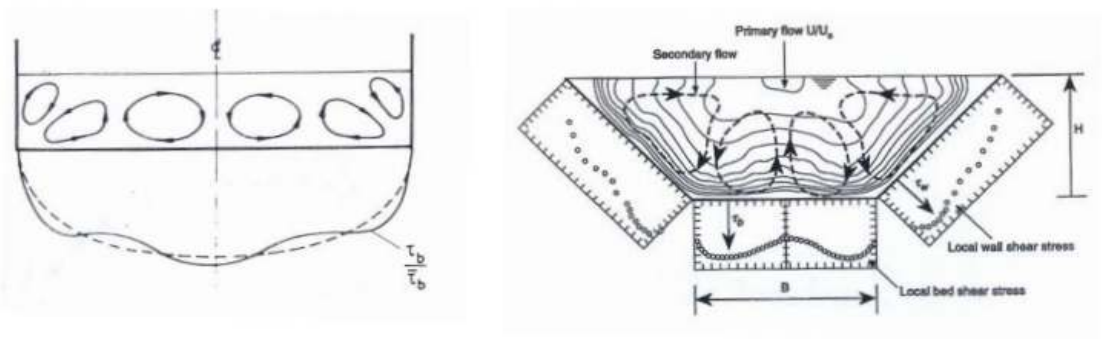


a) Rectangular cross-section (Knight et al., 1983)  b) Trapezoidal cross-section (Knight et al., 1994)

**Fig.1.1 Schematic influence of secondary flow cells on boundary shear distribution**

Compound channel consists of a deep main channel flanked by relatively shallow floodplains on one or both sides of the main channel. During flood when rivers are at high stage, the flow from the main channel spills and spreads to the adjacent floodplain. The reduced hydraulic radius and higher roughness of floodplain result in lower velocities in floodplain as compared to the main channel. The interaction between the faster moving fluid in main channel and slower fluid in floodplain result in a bank of vortices as shown by Knight and Hamed (1984), referred to as "turbulence phenomenon". Consequently there is a lateral transfer of momentum that results in an apparent shear stress at the interface of main channel and floodplain which significantly distort flow and boundary shear stress patterns. The intricate mechanism of momentum transfer in a straight two stage channel is demonstrated in Fig.1.2.

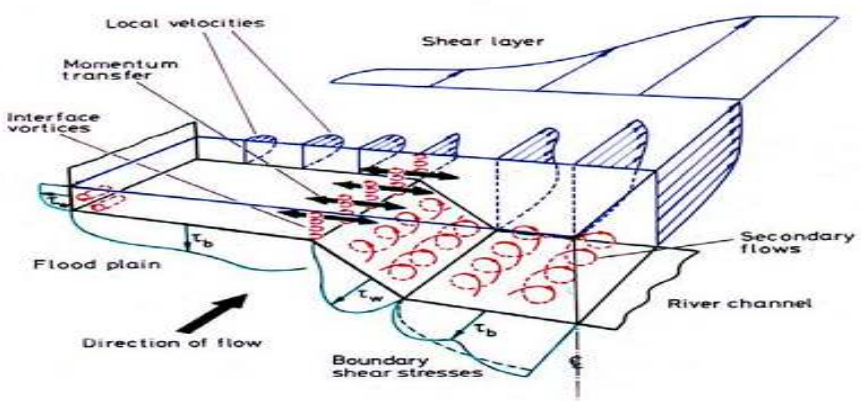


**Fig.1.2 3 D Flow Structures in Open Channel (Shiono and Knight, 1991)**

## 1.3 NUMERICAL MODELLING

Despite of precise results and clear understanding on flow phenomena; experimental approach has some serious drawbacks such as tedious data collection and data can be collected for limited

number of points due to instrument operation constraints; the model is usually not at full scale and the three dimensional flow behavior or some complicated turbulent structure which is the instinct of any open channel flow cannot be effectively captured through experiments. So in these circumstances, computational approach can be adopted to overcome some of these issues and thus provide a complementary tool. In comparison to experimental studies; computational approach is repeatable, can simulate at full scale; can generate the flow taking all the data points into consideration & moreover can take greatest technical challenge *i.e.;* prediction of turbulence. The complex turbulent structures like secondary flow cells, vortices, Reynolds stresses can be effectively and distinctly identified by numerical modeling which are quite essential for energy expenditure studies in open channel flows. Many researchers in the recent years have numerically modeled open channel flows and has successfully validated with the experimental results. Computational Fluid Dynamics (CFD) is a mathematical tool which is used to model open channel ranging from in-bank to over-bank flows. Different models are used to solve Navier-Stokes equations which are the governing equation for any fluid flow. Finite volume method is applied to discretize the governing equations. The accuracy of computational results mainly depends on the mesh quality and the model used to simulate the flow.

## 1.4 OBJECTIVE OF PRESENT STUDY

The present work is aimed to study the distribution of boundary shear stress in simple and compound meandering channels. The distribution of shear stress along the bed and wall of a meandering channel depends on width-depth ratio, relative depth, lateral-longitudinal roughness distribution and sinuosity. Out of these parameters width-depth ratio or aspect ratio and sinuosity plays a major role in estimation of boundary shear stress distribution in meandering channels. Despite immense interest of investigators in

boundary shear stress, no systematic information about the percentage of shear force carried by walls and bed of meandering trapezoidal channel is available. Again one of the features of trapezoidal channels is that there exists an unequal shear drag at the two banks of the channel and this effect becomes more pronounced when the channel is a meandering one. So here it becomes necessary to analyze the inner and outer banks of the meander channel separately, which is yet to gain enough concern from the researchers. Thus an empirical model can be developed for meandering channel to calculate stream wise bed and wall shear stress. And also models can be developed that describes the percentage shear force at inner wall, outer wall and bed separately for trapezoidal meandering channels.

Even for compound meandering channels computational works are reported more than experimental studies. Therefore experimental analysis on distribution of boundary shear stress along the compound meandering channel can be studied more extensively which can further applied to natural rivers during flood conditions. These studies should be useful in determining the actual discharge through a meander channel to solve many hydraulic problems and also it provides a better understanding of flow structure in open meander channels. The objectives of the present work are summarized as:

- Determination of boundary shear stress distribution along the wetted perimeter in simple meandering channels.
- To carry out an investigation concerning the distribution of local shear stress in the main channel and flood plain of meandering compound channel.
- To conduct experiment and analyze experimental data for the investigation of longitudinal wall and bed shear stress for different flow depths for simple and compound meandering channels.

- Development of new mathematical models for evaluation of percentage shear force at wall and bed incorporating meandering effects and to extend the models to the channels of high aspect ratio and sinuosity for meandering channels.
- To validate local shear stress data in terms of shear velocity with 1D model conveyance estimation system (CES) for compound meandering channels.
- To simulate a 60° simple meandering channel for analyzing the flow phenomena such as bed shear stress of a meandering channel by Large Eddy Simulation (LES) model using a CFD tool.

## 1.5 ORGANISATION OF THESIS

The thesis consists of six chapters. General introduction is given in Chapter 1, literature survey is presented in Chapter 2, experimental work is described in Chapter 3, experimental results are outlined and analysis of results are done in Chapter 4, Chapter 5 comprises numerical modeling and finally the conclusions and references are presented in Chapter 6.

General view on rivers and flooding is provided at a glance in the first chapter. Also the chapter introduces the concept of boundary shear distribution in meandering channels. It gives an overview of numerical modeling in open channel flows.

The detailed literature survey by many eminent researchers that relates to the present work from the beginning till date is reported in chapter 2. The chapter emphasizes on the research carried out in straight and meandering channels for both in bank and overbank flow conditions based on boundary shear distribution.

Chapter three describes the experimental programme as a whole. This section explains the experimental arrangements and procedure adopted to obtain observation at different points in

the channel. Also the detailed information about the instrument used for taking observation is given.

The experimental results regarding stage-discharge relationship, boundary shear stress for in bank and overbank flow conditions and mean boundary shear stress are outlined in chapter four. Also this chapter discusses the technique adopted for measuring boundary shear stress. Analyses of the experimental results are done. The analysis of shear force for in bank flow conditions is presented in this chapter

Chapter five presents significant contribution to numerical simulation of in bank channels. The numerical model and the software used within this research are also discussed.

Finally, chapter six summarizes the conclusion reached by the present research and recommendation for the further work is listed out.

References that have been made in subsequent chapters are provided at the end of the thesis.

# LITERATURE SURVEY

## 2.1 GENERAL

Distribution of boundary shear stress along the wetted perimeter of a channel is influenced by many factors notably, the shape of channel cross-section, the longitudinal variation in plan form geometry, the sediment concentration, size and distribution of secondary flow cells and the lateral-longitudinal distribution of wall roughness. It is quite necessary to take into account the general three-dimensional flow structures that exist in open channels to understand the lateral distribution of boundary shear stress. The interaction between the primary longitudinal velocity *U*, and the secondary flow velocities, *V* and *W* are responsible for non-uniform boundary shear distribution in an open channel flow. In earlier times due to 1 Dimensional modeling of flow emphasis was given to local shear stresses and many empirical models were developed regarding the distribution of stream wise component of shear stress. But with time many researchers remarkably noted the presence of secondary velocity in open channel flows due to which complex mixing occurs giving rise to numerous turbulent structures which affects the velocity and shear stress distribution and ultimately the conveyance of the channels. So the present review of literature includes works on experimental research of boundary shear stress for four channel types followed by numerical studies on open channel flow.

## 2.2 PREVIOUS WORKS ON EXPERIMENTAL RESEARCH FOR BOUNDARY SHEAR

The literature review contains a large body of research on the subject of boundary shear stress in open channel flow. This review intends to present some of the selected significant contribution to the study of boundary shear stress in open channel flow. Distribution of shear stress in open channels has been in interest of many investigators from earlier times. Research are done

covering several aspects such as using different channel cross-sections like rectangular and trapezoidal; different channel geometry such as straight, meandering channel, as well as simple and compound channel with different channel surface types like smooth and rough channels to study the factors influencing the boundary shear stress.

### 2.2.1 STRAIGHT SIMPLE CHANNELS

Earlier works on open channel hydraulics involves experiment in simple straight channel having rectangular cross section.

Seven decades ago, Leighly (1932) proposed the idea of using conformal mapping to study the boundary shear stress distribution in open-channel flow. He pointed out that, in the absence of secondary currents, the boundary shear stress acting on the bed must be balanced by the downstream component of the weight of water contained within the bounding orthogonals.

Einstein's (1942) hydraulic radius separation method is still widely used in laboratory studies and engineering practice. Einstein divided a cross-sectional area into two areas $A_b$ and $A_w$ and assumed that the down-stream component of the fluid weight in area $A_b$ is balanced by the resistance of the bed. Likewise, the downstream component of the fluid weight in area $A_w$ was balanced by the resistance of the two side-walls. There was no friction at the interface between the two areas $A_b$ and $A_w$. In terms of energy, the potential energy provided by area $A_b$ was dissipated by the channels bed, and the potential energy provided by area $A_w$ was dissipated by the two side-walls. However he did not propose any method of determining the exact location of division line.

Ghosh and Roy (1970) presented the boundary shear distribution in both rough and smooth open channels of rectangular and trapezoidal sections obtained by direct measurement of

shear drag on an isolated length of the test channel utilizing the technique of three point suspension system suggested by Bagnold. Existing shear measurement techniques were reviewed critically. Comparisons were made of the measured distribution with other indirect estimates, from isovels, and Preston-tube measurements. The discrepancies between the direct and indirect estimates were explained and out of the two indirect estimates the surface Pitot tube technique was found to be more reliable. The influence of secondary flow on the boundary shear distribution was not accurately defined in the absence of a dependable theory on secondary flow.

Kartha and Leutheusser (1970) expressed that the designs of alluvial channels by the tractive force method requires information on the distribution of wall shear stress over the wetted perimeter of the cross-section. The experiments were carried out in a smooth-walled laboratory flume at various aspect ratios of the rectangular cross-section. Wall shear stress measured with Preston tubes were calibrated by a method exploiting the logarithmic form of the inner law of velocity distribution. Results were presented which clearly suggested that none of the present analytical techniques could be counted upon to provide any precise details on tractive force distribution in turbulent channel flow.

Knight and Macdonald (1979) studied that the resistance of the channel bed was varied by means of artificial strip roughness elements, and measurements made of the wall and bed shear stresses. The distribution of velocity and boundary shear stress in a rectangular flume was examined experimentally, and the influence of varying the bed roughness and aspect ratio were accessed. Dimensionless plots of both shear stress and shear force parameters were presented for different bed roughness and aspect ratios, and those illustrated the complex way in which such parameters varied. The definition of a wide channel was also examined, and a graph giving the

limiting aspect ratio for different roughness conditions was presented. The boundary shear stress distributions and isovel patterns were used to examine one of the standard side-wall correction procedures. One of the basic assumptions underlying the procedure was found to be untenable due to the cross channel transfer of linear momentum.

Knight (1981) proposed an empirically derived equation that presented the percentage of the shear force carried by the walls as a function of the breadth/depth ratio and the ratio between the Nikuradse equivalent roughness sizes for the bed and the walls. The results were compared with other available data for the smooth channel case and some disagreements noted. The systematic reduction in the shear force carried by the walls with increasing breadth/depth ratio and bed roughness was illustrated. Further equations were presented giving the mean wall and bed shear stress variation with aspect ratio and roughness parameters. Although the experimental data was somewhat limited, the equations were novel and indicated the general behaviour of open channel flows with success. This idea was further discussed by Noutsopoulos and Hadjipanos (1982).

Knight and Patel (1985) reported some of the laboratory experiments results concerning the distribution of boundary shear stresses in smooth closed ducts of a rectangular cross section for aspect ratios between 1 and 10. The distributions were shown to be influenced by the number and shape of the secondary flow cells, which, in turn, depended primarily upon the aspect ratio. For a square cross section with 8 symmetrically disposed secondary flow cells, a double peak in the distribution of the boundary shear stress along each wall was shown to displace the maximum shear stress away from the centre position towards each corner. For rectangular cross sections, the number of secondary flow cells increased from 8 by increments of 4 as the aspect

ratio increased, causing alternate perturbations in the boundary shear stress distributions at positions where there were adjacent contra-rotating flow cells. Equations were presented for the maximum, centreline and mean boundary shear stresses on the duct walls in terms of the aspect ratio.

Knight and Sterling(2000) observed the distribution of boundary shear stress in circular conduits flowing partially full with and without a smooth flat bed for a data ranging from 0.375<F<1.96 and 6.5*104<R<3.42*105, using Preston-tube technique. The distribution of boundary shear stress is shown to depend on geometry and Froude no. The results have been analysed in terms of variation of local shear stress with perimetric distance and the percentage of total shear force acting on wall or bed of the conduit. The $\%SF_W$ results have been shown to agree well with Knight's (1981) empirical formula for prismatic channels. The interdependency of secondary flow and boundary shear stress has been established and its implications for sediment transport have also been examined.

Yang and McCorquodale (2004) developed a method for computing three-dimensional Reynolds shear stresses and boundary shear stress distribution in smooth rectangular channels by applying an order of magnitude analysis to integrate the Reynolds equations. A simplified relationship between the lateral and vertical terms was hypothesized for which the Reynolds equations become solvable. This relationship was in the form of a power law with an exponent of n = 1, 2, or infinity. The semi-empirical equations for the boundary shear distribution and the distribution of Reynolds shear stresses were compared with measured data in open channels. The power-law exponent of 2 gave the best overall results while n = infinity gave good results near the boundary.

Guo and Julien (2005) proposed a method to determine average bed and sidewall shear stresses in smooth rectangular open-channel flows after solving the continuity and momentum equations. The analysis showed that the shear stresses were functions of three components: (1) gravitational; (2) secondary flows; and (3) interfacial shear stress. An analytical solution in terms of series expansion was obtained for the case of constant eddy viscosity without secondary currents. In comparison with laboratory measurements, it slightly overestimated the average bed shear stress measurements but underestimated the average sidewall shear stress by 17% when the width–depth ratio becomes large. A second approximation was formulated after introducing two empirical correction factors. The second approximation agreed very well ($R^2 > 0.99$ and average relative error less than 6%) with experimental measurements over a wide range of width–depth ratios.

Lashkar and Fathi (2010) conducted experiments to determine the contribution of wall shear force on total boundary shear force. A nonlinear regression-based technique was carried out to analyze the results and develop equations to determine the percentage of wall and bed shear force on the wetted perimeter of the rectangular channels.

### 2.2.2 STRAIGHT COMPOUND CHANNEL

Zheleznyakov (1965) was probably the first to investigate the interaction between the main channel and the adjoining floodplain. He demonstrated under laboratory conditions the effect of momentum transfer mechanism, which was responsible for decreasing the overall rate of discharge for floodplain depths just above the bank full level. As the floodplain depth increased, the importance of the phenomena diminished.

Ghosh and Jena (1973) and Ghosh and Mehata (1974) reported studies on boundary shear distribution in straight two stage channels for both smooth and rough boundaries. They found the distribution of shear is non-uniform and the location of maximum bed and side shear to be some distance from the centreline and free surface. They related the sharing of the total drag force by different segments of the channel section to the depth of flow and roughness concentration.

Myers and Elswy (1975) studied the effect of interaction mechanism and shear stress distribution in channels of complex sections. In comparison to the values under isolated condition, the results showed a decrease up to 22 percent in channel shear and increase up to 260 percent in floodplain shear. This indicated the possible regions of erosion and scour of the channel and flow distribution in alluvial compound sections.

Rajaratnam and Ahmadi (1979) studied the flow interaction between straight main channel and symmetrical floodplain with smooth boundaries. The results demonstrated the transport of longitudinal momentum from main channel to flood plain. Due to flow interaction, the bed shear in floodplain near the junction with main channel increased considerably and that in the main channel decreased. The effect of interaction reduced as the flow depth in the floodplain increased.

Wormleaton, Alen, and Hadjipanos (1982) undertook a series of laboratory tests in straight channels with symmetrical floodplains and used "divide channel" method for the assessment of discharge. From the measurement of boundary shear, apparent shear stress at the vertical, horizontal, and diagonal interface plains originating from the main channel-floodplain junction could be evaluated. An apparent shear stress ratio was proposed which was found to be a useful yardstick in selecting the best method of dividing the channel for calculating discharge.

It was found that under general circumstances, the horizontal and diagonal interface method of channel separation gave better discharge results than the vertical interface plain of division at low depths of flow in the floodplains.

Knight and Demetriou (1983) conducted experiments in straight symmetrical compound channels to understand the discharge characteristics, boundary shear stress and boundary shear force distributions in the section. They presented equations for calculating the percentage of shear force carried by floodplain and also the proportions of total flow in various sub-areas of compound section in terms of two dimensionless channel parameters. For vertical interface between main channel and floodplain the apparent shear force was found to be more at low depths of flow and also for high floodplain widths. On account of interaction of flow between floodplain and main channel, it was found that the division of flow between the sub-areas of the compound channel did not follow the simple linear proportion to their respective areas.

Knight and Hamed (1984) extended the work of Knight and Demetriou (1983) to rough floodplains. The floodplains were roughened progressively in six steps to study the influence of different roughness between floodplain and main channel to the process of lateral momentum transfer. Using four dimensionless channel parameters, they presented equations for the shear force percentages carried by floodplains and the apparent shear force in vertical, horizontal, diagonal, and bisector interface plains. The apparent shear force results and discharge data provided the strength and weakness of these four commonly adopted design methods used to predict the discharge capacity of the compound channel.

### 2.2.3 MEANDER SIMPLE CHANNELS

In bank flows in meandering channel are highly three dimensional and exhibit complex turbulent structures like secondary motions. The phenomenon of secondary motion was first given by Boussinesq (1868) and Thomson (1876). They studied the influence of secondary motion on primary velocity distribution. Later on Jia *et.al*., 2001 showed that secondary motion occurs due to the imbalance between the driving centrifugal force and the transverse pressure gradient.

Knight, Yuan and Fares (1992) reported the experimental data of SERC-FCF concerning boundary shear stress distributions in meandering channels throughout the path of one complete wave length. They also reported the experimental data on surface topography, velocity vectors, and turbulence for the two types of meandering channels of sinuosity 1.374 and 2.043 respectively. They examined the effects of secondary currents, channel sinuosity, and cross section geometry on the value of boundary shear in meandering channels and presented a momentum-force balance for the flow.

Shiono, Muto, Knight and Hyde (1999) presented the experimental data of secondary flow and turbulence using two components Laser- Doppler Anemometer for both straight and meandering channels to understand the flow mechanism in meandering channels. They developed turbulence models and studied the behaviour of secondary flow and centrifugal forces for both in-bank and over-bank flow conditions. They investigated the energy loss due to boundary friction, secondary flow, turbulence, expansion and contraction in meandering channels.

### 2.2.4 MEANDER COMPOUND CHANNEL

Flow in compound channel often inundate the adjacent floodplains due to lateral momentum transfer takes place at the main channel and floodplain interface, which generates more complicated flow structures than in simple meander channel. Compared to the extensive literature for straight compound channel, much less work has been reported for compound meandering channel flows.

Ghosh and Kar (1975) studied the evaluation of interaction effect and the distribution of boundary shear stress in meander channel with floodplain. Using the relationship proposed by Toebes and Sooky (1967) they evaluated the interaction effect by a parameter (*W*). The interaction loss increased up to a certain floodplain depth and there after it decreased. They concluded that the channel geometry and roughness distribution did not have any influence on the interaction loss.

Ervine, Alan, Koopaei, and Sellin (2000) presented a practical method to predict depth-averaged velocity and shear stress for straight and meandering over bank flows. They also presented an analytical solution to the depth-integrated turbulent form of the Navier-Stokes equation that includes lateral shear and secondary flows in addition to bed friction. They applied this analytical solution to a number of channels, at model, and field scales, and compared with other available methods such as that of Shiono and Knight and the lateral distribution method (LDM).

Patra and Kar (2000) reported the test results concerning the boundary shear stress, shear force, and discharge characteristics of compound meandering river sections composed of a

rectangular main channel and one or two floodplains disposed off to its sides. They used five dimensionless channel parameters to form equations representing the total shear force percentage carried by floodplains. A set of smooth and rough sections were studied with aspect ratio varying from 2 to 5. Apparent shear forces on the assumed vertical, diagonal, and horizontal interface plains were found to be different from zero at low depths of flow and the sign changes with increase in depth over floodplain. They proposed a variable-inclined interface for which apparent shear force was calculated as zero. They presented empirical equations for predicting proportion of discharge carried by the main channel and floodplain.

Patra and Kar (2004) reported the test results concerning the flow and velocity distribution in meandering compound river sections. Using power law they presented equations concerning the three-dimensional variation of longitudinal, transverse, and vertical velocity in the main channel and floodplain of meandering compound sections in terms of channel parameters. The results of formulations compared well with their respective experimental channel data obtained from a series of symmetrical and unsymmetrical test channels with smooth and rough surfaces. They also verified the formulations against the natural river and other meandering compound channel data.

Khatua (2008) extended the work of Patra and Kar (2000) to meandering compound channels. Using five parameters (sinuosity $S_r$, amplitude, relative depth, width ratio and aspect ratio), general equations representing the total shear force percentage carried by floodplain was presented. The proposed equations are simple, quite reliable and gave good results with the observed data for straight compound channel of Knight and Demetriou (1983) as well as for the meandering compound channel.



Khatua (2010) reported the distribution of boundary shear force for highly meandering channels having distinctly different sinuosity and geometry. Based on the experimental results, the interrelationship between the boundary shear, sinuosity and geometry parameters has been shown. The models are also validated using the well published data of other investigators.

## 2.3 OVERVIEW OF NUMERICAL MODELLING ON OPEN CHANNEL FLOW

For the past three decades, flow in simple and compound meandering channels has been extensively studied both experimentally and numerically. Various numerical models such as standard k-ε model, non-linear k-ε model, k-ω model, algebraic Reynolds stress model (ASM), Reynolds stress model (RSM) and large eddy simulation (LES) have been developed to simulate the complex secondary structure in compound meandering channel. The standard k- ε model is an isotropic turbulence closure but fails to reproduce the secondary flows. Although nonlinear k-ε model can simulate secondary currents successfully in a compound channel, it cannot accurately capture some of the turbulence structures. ASM is economical because it uses adhoc expressions to solve Reynolds stress transport equations. But the simulated results by ASM found to be unreliable. Reynolds stress model (RSM) computes Reynolds stresses by directly solving Reynolds stress transport equation but its application to open channel is still limited due to the complexity of the model. Large eddy simulation (LES) solves spatially-averaged Navier-Stokes equation. Large eddies are directly resolved, but eddies smaller than mesh are modelled. Though LES is computationally expensive to be used for industrial application but can efficiently model nearly all eddy sizes.

Cokljat and Younis and Basara and Cokljat (1995) proposed the RSM for numerical simulations of free surface flows in a rectangular channel and in a compound channel and found good agreement between predicted and measured data.

Thomas and Williams (1995) describes a Large Eddy Simulation of steady uniform flow in a symmetric compound channel of trapezoidal cross-section with flood plains at a Reynolds number of 430,000. The simulation captures the complex interaction between the main channel and the flood plains and predicts the bed stress distribution, velocity distribution, and the secondary circulation across the floodplain. The results are compared with experimental data from the SERC Flood Channel Facility at Hydraulics Research Ltd, Wallingford, England

Salvetti et al. (1997) has conducted LES simulation at a relatively large Reynolds number for producing results of bed shear, secondary motion and vorticity well comparable to experimental results.

Rameshwaran P, Naden PS.(2003) analyzed three dimensional nature of flow in compound channels.

Sugiyama H, Hitomi D, Saito T.(2006) used turbulence model consists of transport equations for turbulent energy and dissipation, in conjunction with an algebraic stress model based on the Reynolds stress transport equations. They have shown that the fluctuating vertical velocity approaches zero near the free surface. In addition, the compound meandering open channel is clarified somewhat based on the calculated results. As a result of the analysis, the present algebraic Reynolds stress model is shown to be able to reasonably predict the turbulent flow in a compound meandering open channel.

Kang H, Choi SU. (2006) used a Reynolds stress model for the numerical simulation of uniform 3D turbulent open-channel flows. The developed model is applied to a flow at a Reynolds number of 77000 in a rectangular channel with a width to depth ratio of 2. The simulated mean flow and turbulence structures are compared with measured and computed data from the literature. It is found that both production terms by anisotropy of Reynolds normal stress and by Reynolds shear stress contribute to the generation of secondary currents.

Jing, Guo and Zhang (2008) simulated a three-dimensional (3D) Reynolds stress model (RSM) for compound meandering channel flows. The velocity fields, wall shear stresses, and Reynolds stresses are calculated for a range of input conditions. Good agreement between the simulated results and measurements indicates that RSM can successfully predict the complicated flow phenomenon.

Cater and Williams (2008) reported a detailed Large Eddy Simulation of turbulent flow in a long compound open channel with one floodplain. The Reynolds number is approximately 42,000 and the free surface was treated as fully deformable. The results are in agreement with experimental measurements and support the use of high spatial resolution and a large box length in contrast with a previous simulation of the same geometry. A secondary flow is identified at the internal corner that persists and increases the bed stress on the floodplain.

Kim et al. (2008) analyses three-dimensional flow and transport characteristics in two representative multi-chamber ozone contactor models with different chamber width using LES.

Wang *et.al*., (2008) used different turbulence closure schemes i.e., the mixing-length model and the $k$-$\varepsilon$ model with different pressure solution techniques i.e., hydrostatic assumptions

and dynamic pressure treatments are applied to study the helical secondary flows in an experiment curved channel. The agreements of vertically-averaged velocities between the simulated results obtained by using different turbulence models with different pressure solution techniques and the measured data are satisfactory. Their discrepancies with respect to surface elevations, super elevations and secondary flow patterns are discussed.

Balen et.al., (2010) performed LES for a curved open-channel flow over topography. It was found that, notwithstanding the coarse method of representing the dune forms, the qualitative agreement of the experimental results and the LES results is rather good. Moreover, it is found that in the bend the structure of the Reynolds stress tensor shows a tendency toward isotropy which enhances the performance of isotropic eddy viscosity closure models of turbulence.

Beaman (2010) studied the conveyance estimation using LES method.

Esteve *et.al.,* (2010) simulated the turbulent flow structures in a compound meandering channel by Large Eddy Simulations (LES) using the experimental configuration of Muto and Shiono (1998). The Large Eddy Simulation is performed with the in-house code LESOCC2. The predicted stream wise velocities and secondary current vectors as well as turbulent intensity are in good agreement with the LDA measurements.

Ansari *et.al*., (2011) presented the use of (CFD) to determine the distribution of the bed and side wall shear stresses in trapezoidal channels. The impact of the variation of the slant angles of the side walls, aspect ratio and composite roughness on the shear stress distribution is analyzed. These equations derived compute the shear stress as a function of three components. The results show a significant contribution from the secondary currents and internal shear

stresses on the overall shear stress at the boundaries. This work also extends previous work of the authors on rectangular channels.

Larocque, Imran, Chaudhry (2013) presented 3D numerical simulation of a dam-break flow using LES and k- ε turbulence model with tracking of free surface by volume-of-fluid model. Results are compared with published experimental data on dam-break flow through a partial breach as well as with results obtained by others using a shallow water model. The results show that both the LES and the k –ε modeling satisfactorily reproduce the temporal variation of the measured bottom pressure. However, the LES model captures better the free surface and velocity variation with time.

From literature survey, it is found that very limited work on boundary shear stress has been reported for meandering channels. Although adequate literature is available on numerical studies that make use of different turbulence models for modeling compound meandering channels but the literature lacks substantial experimental works for compound meandering channels.

# EXPERIMENTAL SETUP AND PROCEDURE

## 3.1. GENERAL

Estimation of boundary shear stress in a meandering channel is typical in the sense that many unseen flow parameters comes into play due to which the three-dimensional nature of flow increases. Also it is established by many researchers that the secondary current affects the distribution of boundary shear stress in open channel flow. Owing to this the evaluation of discharge capacity in a meandering channel is a complicated process and is dependent on precise prediction of shear force carried by different boundary elements of a channel. The present research work utilises the flume facility available in the Fluid Mechanics and Hydraulic Engineering Laboratory of the Civil Engineering Department at the National Institute of Technology, Rourkela, India. The basic objective behind these experiments is to conceive better understanding on the variation of distribution of boundary shear stress due to variation of flow and sinuosity under uniform flow conditions. The following section provides a brief overview of details of hydraulic and geometric parameters of the present meandering channel, experimental arrangements, measuring equipments and procedure used in the process of data collection.

## 3.2 EXPERIMENTAL ARRANGEMENTS

### *3.2.1 Apparatus and Materials Used*

The experiments are conducted in channel built in a long tilting flume made up metal frame with glass walls of size 15m long; 4m wide and 0.5m deep. The flume can be tilted with the help of hydraulic jack arrangement for different bed slope arrangements. The channel is cast using 6mm thick Perspex sheet, having Manning's n value 0.01. The experimental meandering channel is

trapezoidal at cross-section and all measurements were taken at central bend apex. The detailed information on geometric parameters of meandering channel is provided in the table below.

**Table.1 Geometry Parameters of the Experimental Meandering Channel**

| Sl. No. | Item Description | Highly Meander channel |
|---|---|---|
| 1. | Wave length in down valley direction | 4054mm |
| 2. | Amplitude | 2027mm |
| 3. | Geometry of main channel section | Trapezoidal (side slope 1:1) |
| 4. | Main channel width ($B$) | 330mm at bottom |
| 5. | Bank full depth of main channel | 65mm |
| 6. | Top width of compound channel ($B'$) | 460 mm |
| 7. | Slope of the channel | 0.0055 |
| 8. | Meander belt width ($B_W$) | 2357mm |
| 9. | Nature of surface bed | Smooth and rigid bed |
| 10. | Sinuosity($S_r$) | 2.04 |
| 11. | Cross over angle in degree | 90 |
| 12. | Flume size | 15m*4m*0.5m |

Photographs of the experimental meandering channel from two different views with measuring equipments are shown in Photos.3.1 (a, b) whereas Figs.3.1 (a, b) show the plan view of half meander wavelength with dimensional details at bed and at bank full level (i.e., at 6.5 cm) respectively.

**Photo.3.1 (a) View of Experimental Channel**

**Photo.3.1 (b) Side View of Experimental Channel**

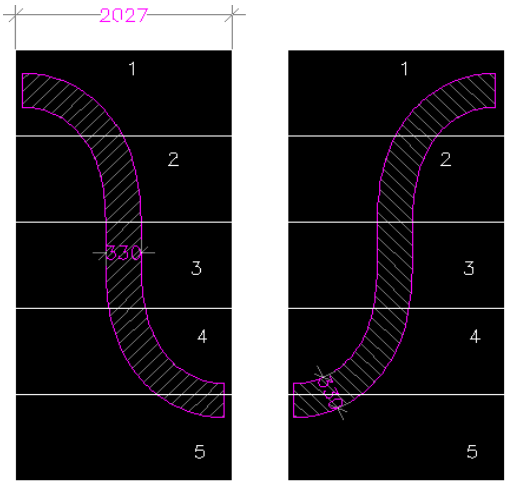


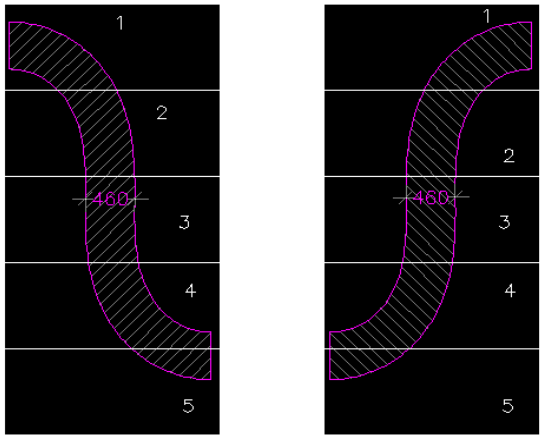


**Fig.3.1(a) At Bed Level** **Fig.3.1(b) At 6.5cm above Bed**

For the sake of experiment, two tanks namely overhead tank made up of reinforced cement concrete (RCC) and masonry volumetric tank at the downstream of the channel are constructed. Various arrangements are done within the flume to convey water to the channel. Those are stilling chamber, baffle walls, head gate, rectangular notch, square wire mesh, travelling bridge and tail gate. The experimental arrangements also consists of an underground sump, water supply devices, two parallel pumps etc. The plan view of full length experimental channel with other arrangements is shown in Fig.3.2.

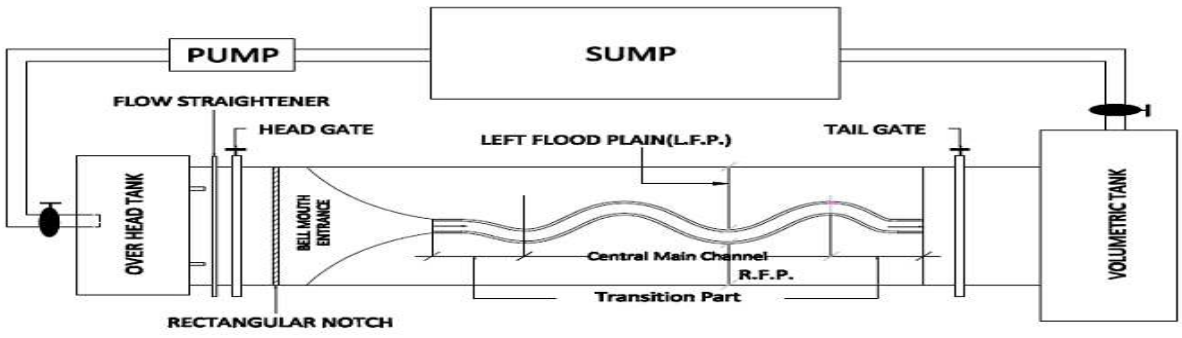


**Fig.3.2 *Schematic Diagram of Experimental Setup**

**After Mohanty et.al. (2012)*

### *3.2.2 Measuring Equipments*

A pointer gauge, located on a mobile instrument carriage, is used to measure the water level at different locations along the flume to an accuracy of 0.1 mm. Five unequally spaced micro-Pitot tube each of them having 4.6 mm external diameter is used in conjunction with five manometers placed inside a transparent fibre block fixed to a wooden board. A spirit level is positioned at the top of the wooden board to maintain the verticality of manometers. On the experimental flume, main guide rails are provided on which a travelling bridge is moved in the longitudinal direction of the entire experimental channel. The point gauge and a micro-Pitot tube are attached to the travelling bridge with secondary guide rails allowing the equipments to move in both longitudinal and the transverse direction of the experimental channel. A rectangular notch arrangement made at the upstream of the channel is calibrated to establish stage-discharge relationship and to estimate the theoretical discharge whereas a piezometer fitted to the tail tank for actual discharge through the channel. The measuring equipments and the devices are arranged and calibrated properly to carry out experiments in the channel. The following photographs show the measuring devices used for data collection. The photographs of series of pitot static tube fitted to stand with point gauge and set of piezometers fitted to wooden board to record pressure with spirit level are shown in Photos. 3.2(a) and 3.4(b) respectively.

**Photo 3.2(a) Series of Pitot static tube** **Photo .3.2(b) Set of piezometers with spirit level**

## 3.3 EXPERIMENTAL PROCEDURE

Two parallel pumps are used to pump water at the rate up to 200 lit/sec from an underground sump to the overhead tank. The water in overhead tank is maintained at constant head so that the excess water returns to the sump again. The water is conveyed to the flume by two different supply pipelines. To reduce large disturbances in the outgoing flow from the pumps, water is first conducted into a stilling tank from where it is led to an adjustable vertical gate along with series of baffle walls in upstream section sufficiently ahead of rectangular notch to reduce turbulence and velocity of the incoming water. From the rectangular notch water is made to fall on a wire mesh provided just below the notch. Water is then directed to the channel to flow under gravity through a smooth bell mouth transition section to improve the inflow conditions from the inlet tank to a specific channel. Finally the water at the downstream end is allowed to flow through another adjustable tailgate and is collected in a masonry volumetric tank from where it is again flow back to the underground sump. From the sump, water is then pumped back to the overhead tank, thus a complete re-circulating system of water supply for the experimental channel is established. The adjustable tailgates were used to achieve uniform flow for a specific

flow depth. Since in uniform flow conditions, the energy slope ($S_e$), the water surface slope ($S_w$) and the bed slope ($S_0$) are all equal, i.e; $S_e = S_w = S_0$. It is only under this condition that the depth and velocity can be assumed to be constant at all cross sections, before any measurement could be taken in the channel, uniform flow conditions had to be achieved. The adjustable tailgates at the downstream end of the flume were used for this purpose. All the measurements are taken at the bend apex of the third wave reach of the experimental channel from the upstream end to achieve a fully developed flow. Observations are recorded for different flow depths, only under steady and uniform conditions.

### *3.3.1 Measurement of Bed Slope*

The water in the channel is kept still by blocking the adjustable tail gate provided at the downstream end of experimental channel. With the help of a pointer gauge the bed and water surface level are recorded at a certain point (say A) in standstill condition of water. Towards downstream, at another point (say B) the bed and water surface level are again noted. The elevation between these two points is given by ($\Delta A$ - $\Delta B$). This is repeated for number of points along the channel centerline for distance of one wavelength. The mean slope for the meandering channels may be obtained from,

$$Slope = \Sigma(\Delta A - \Delta B) / L \qquad (1)$$

Where,

$\Delta A$ = Level difference of channel bed and water surface at point A

$\Delta B$ = Level difference of channel bed and water surface at point B

L = length of meander wave along the centerline.

### *3.3.2 Calibration of Notch*

The accurate estimation of discharge can be obtained from the rectangular notch fitted at the upstream of the channel. For which the notch is needed to be calibrated first before measuring the discharge. The actual discharge passing through channel is recorded from a volumetric tank of 208666 $cm^2$ provided at outfall of the channel. A piezometer connected to this tank gives rise in height of water in volumetric tank over a time interval. Variation of time depends on the rate of flow from the channel e.g., the time of collection of water in the measuring tanks vary between 60 to 300 seconds; lower one for higher rate of discharge. Time is recorded using a stopwatch with respect to the collection of water in the tank and the rise in height of water is obtained from measuring scale attached to the piezometer. Finally change in the mean water level in the tank over the time interval is recorded. The volume of water collected in the tank is given by

$$V = Ah \qquad (2)$$

From the knowledge of the volume of water collected in the measuring tank and the corresponding time of collection, the actual discharge in the experimental channel for each run is obtained by,

$$Q_a = V/t \qquad (3)$$

For theoretical discharge, the height of water above notch is measured by a point gauge arrangement made at the notch in a wooden platform. Theoretical discharge is given by,

$$Q_a = C_d \frac{2}{3} L\sqrt{2g} H_n^{3/2} \qquad (4)$$

The coefficient of discharge for each run is calculated as per equation given below,

$$Q_a = C_d Q_t \tag{5}$$

Where $A$ = Area of volumetric tank i.e., 208666 cm$^2$, $h$ = Height of water in the volumetric tank, $Q_a$ = Actual discharge, $V$ = volume of water in tank, $t$ = time interval, $Q_t$ = Theoretical discharge, $L$ = Length of the notch, $H_n$ = Height of water above the notch, $g$ = Acceleration due to gravity, $C_d$ = Coefficient of discharge calculated from notch calibration

Hence the rectangular notch is calibrated for the purpose of present experiment and the coefficient of discharge $C_d$ is found to be 0.71.

### *3.3.3 Measurement of Normal Depth and Discharge*

Once the notch is calibrated and the coefficient of discharge is made fixed, the discharge '$Q_a$' for each run is calculated as for the equation given below.

$$Q_a = C_d \frac{2}{3} L\sqrt{2g} H_n^{3/2} \tag{6}$$

where

$Q_a$ = Actual discharge

$C_d$ = Coefficient of discharge calculated from notch calibration

$L$ = Length of the notch

$H_n$ = Height of water above the notch

$g$ = Acceleration due to gravity.

Experimental results concerning stage-discharge relationships for meandering channels with rigid

boundaries are accessed. A pointer gauge located on the travelling bridge was used to measure the flow depth at bend apex in the channel for a given discharge. For meandering channel, the level difference of bed and water surface at outer bank is recorded by pointer gauge which gives depth at the outer bank. Likewise the procedure is repeated at inner bank to get normal depth. The mean depth of these two depths is taken as normal depth for a particular discharge.

# EXPERIMENTAL RESULTS AND ANALYSIS

## 4.1 GENERAL

The experimental results concerning the distribution of boundary shear along the wetted perimeter and flow has been presented in this section. The stage-discharge relationship from in-bank to over-bank flow situation for meandering compound channel is shown in Fig.4.1. Analysis of results is done for distribution of boundary shear stress in meandering channels and shear force results are derived accordingly. Empirical models are developed for percentage of shear force carried by bed and inner and outer banks to better understand the underlying flow mechanism in meandering channels.

## 4.2 STAGE- DISCHARGE RELATIONSHIP

Making a flood prediction while using hydraulic model which incorporates various flow features, is not an easy task. Researches have shown that the structures of the flow are even more difficult to analyze for compound meandering channel, due to an increase in 3-Dimensional nature of flow (Shiono, Al-Romaih, and Knight 1999). In the present experimentation involving flow in simple meandering channel, steady and uniform flow has been tried to achieve. Flow depths in the experimental channel runs are so maintained that the water surface slope becomes parallel to the valley slope to minimize the energy losses. Under such conditions, the depths of flow at the channel centerline along one wave reach must be the same. This depth of flow is considered as normal depth, which can carry a particular flow only steady and uniform condition. The stage discharge curve plotted for the present meandering channel is shown in Fig.4.1 The figure show

discharge against the stage from in-bank to over-bank flow situations. Also the hydraulic parameters of each experimental runs for in bank and overbank flow are listed in Table 2.

**Table 2. Hydraulic parameter for the experimental runs**

| Runs | Discharge Q (in lit/s) | Flow depth (in cm) | Relative depth β | Froude No. ($F_r$) | Reynolds No. (R) |
|---|---|---|---|---|---|
| ***INBANK FLOW*** | | | **(H/h)** | | |
| 1 | 1.165 | 1.7 | 0.2615 | 0.495 | 3847.90 |
| 2 | 1.872 | 2.5 | 0.3846 | 0.441 | 5832.49 |
| 3 | 3.803 | 3.8 | 0.5846 | 0.468 | 10851.62 |
| 4 | 4.153 | 4.0 | 0.6154 | 0.471 | 11701.64 |
| 5 | 6.055 | 5.0 | 0.7692 | 0.484 | 16035.97 |
| 6 | 7.5 | 5.8 | 0.8923 | 0.473 | 18953.12 |
| ***OVERBANK FLOW*** | | | **(H'-h /H')** | | |
| 1 | 18.564 | 8.9 | 0.2697 | 0.314314 | 28389.52 |
| 2 | 33.227 | 9.5 | 0.3158 | 0.397014 | 39091.89 |
| 3 | 42.513 | 9.9 | 0.3434 | 0.464403 | 46843.45 |
| 4 | 46.635 | 10.1 | 0.3564 | 0.495639 | 53654.54 |
| 5 | 52.533 | 10.6 | 0.3868 | 0.521894 | 62962.90 |

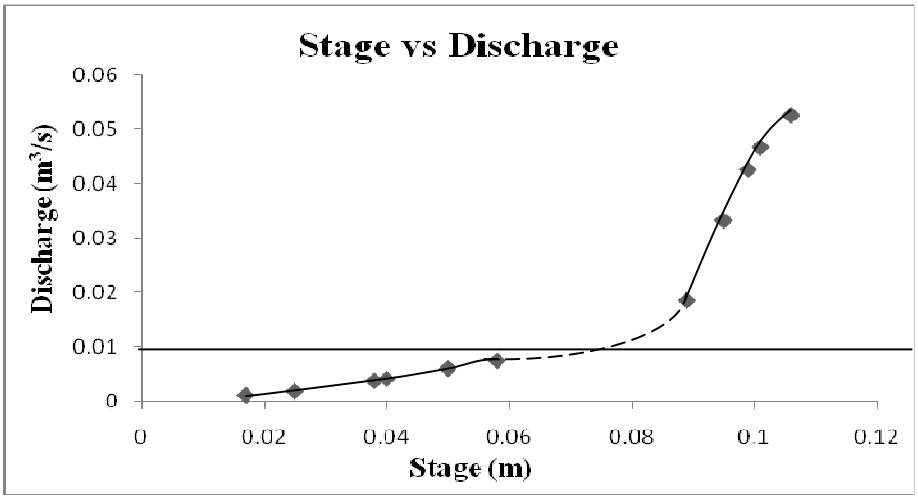


**Fig.4.1 Plot of Stage versus Discharge**

## 4.3 SHEAR STRESS MEASUREMENTS

Shear studies in open channel flow has many implications such as bed load transport, channel migration, momentum transfer etc. Bed shear forces are useful for the study of bed load transfer where as wall shear forces presents a general view of channel migration pattern. There are several methods used to evaluate bed and wall shear stress in an open channel. The Preston-tube method is an indirect estimate for shear stress measurements and is widely used for experimental channel which is described below. In the following section, results regarding the distribution of boundary shear stress along with the contours of local shear stress is shown and discussed. Also the mean boundary shear stress results are discussed in details.

### *4.3.1 Preston-tube Technique*

Using Preston's technique (1954) together with calibration curves of Patel's (1965) local boundary shear stress measurements were made around wetted perimeter of the present meandering channel. Preston developed a simple shear stress measurement technique for smooth boundaries in a fully developed turbulent flow using a Pitot tube. Based on the law of the wall assumption (Bradshaw and Huang, 1995), i.e. the velocity distribution near the wall can be empirically related to the differential pressure between the dynamic and static pressures,

Preston presented a non-dimensional relationship between the differential pressures, $\Delta P$ and the boundary shear stress, $\tau_o$:

$$\left(\frac{\tau_0 d^2}{4\rho v^2}\right) = F\left(\frac{\Delta P}{4\rho v^2}\right) \qquad (7)$$

Where, $d$ is the outside diameter of the tube, $\rho$ is the density of the flow, $v$ is the kinematic viscosity of the fluid and $F$ is an empirical function. Following this work, Patel (1965) presented definitive calibration curves for the Preston tube defined in terms of two non-dimensional parameters which are used to convert pressure readings to boundary shear stress:

$$x^* = \log_{10}(\Delta P d^2/4\rho v^2)\,, \qquad y^* = \log_{10}(\tau_0 d^2/4\rho v^2) \tag{8}$$

The calibration of $x^*$and $y^*$ for different regions of the velocity distribution (i.e. viscous sub layer, buffer layer and logarithmic layer) is expressed by three different formulae:

$$y^* = 0.5x^* + 0.037 \qquad \text{for } 0 < y^* < 1.5$$

$$y^* = 0.8287 - 0.1381x^* + 0.1437x^{*2} - 0.006x^{*3} \qquad \text{for } 1.5 < y^* < 3.5$$

$$x^* = y^* + 2\log_{10}(1.95y^* + 4.1) \qquad \text{for } 3.5 < y^* < 5.3$$

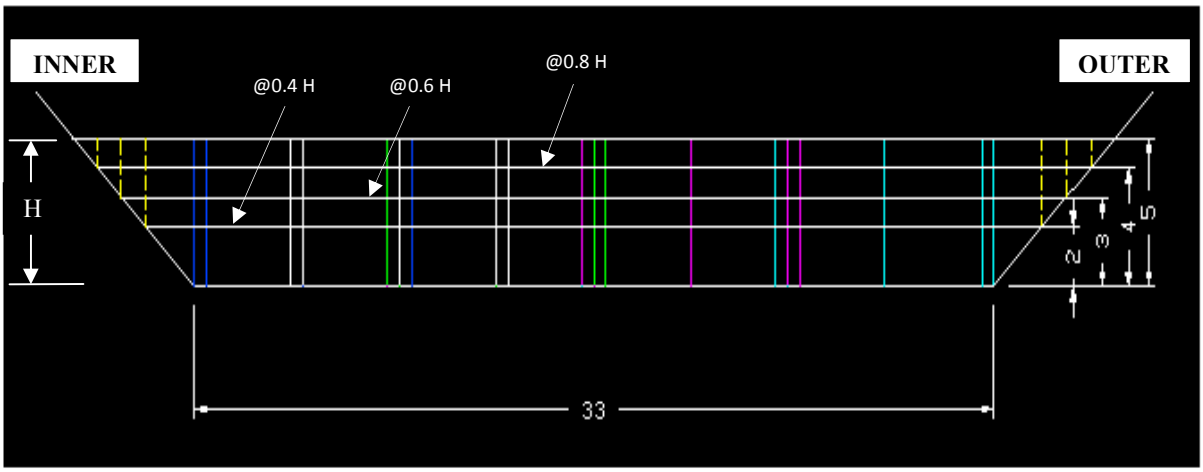


**Fig 4.2 (a) Definition sketch of point locations used in shear stress measurements for simple meander channel at bend apex (All location spacing's are in centimeters)**

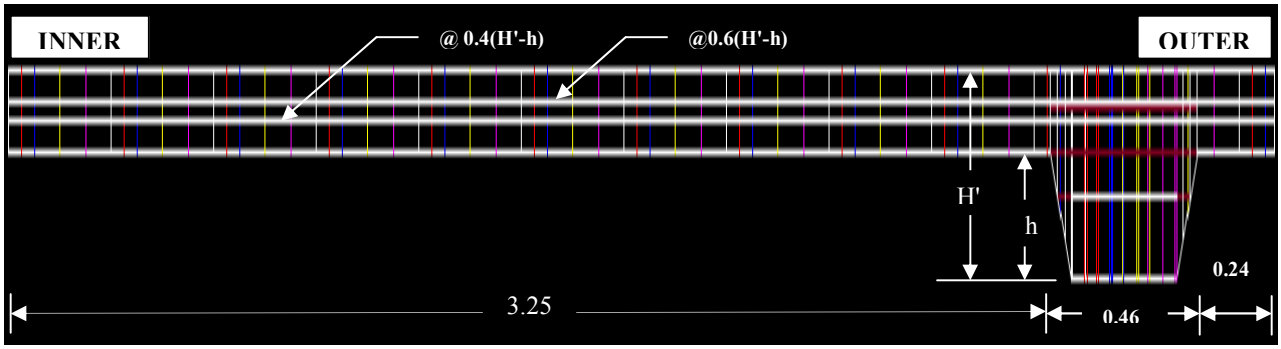


**Fig 4.2 (b) Definition sketch of point locations used in shear stress measurements for compound meander channel at bend apex (All location spacing's are in meters)**

In the present case, all shear stress measurements are taken at the bend apex due to minimum curvature effect. The pressure readings were taken using Pitot tube. These are placed at the predefined points of the flow-grid in the channel, facing the flow which is demonstrated in Fig. 4.2. (a) and 4.2 (b) for in bank and overbank flow conditions respectively. The manometers attached to the respective Pitot tubes are used to measure head difference. The differential pressure was then calculated from the readings on the vertical manometer:

$$\Delta P = \rho g \Delta h$$

Where $\Delta h$ is the difference between the two readings from the dynamic and static, $g$ is the acceleration due to gravity and $\rho$ is the density of water. Here the tube coefficient is taken as unit and the error due to turbulence considered negligible while measuring velocity. Each experimental runs of the channel are carried out by maintaining the water surface slope parallel to the valley slope to achieve the steady and uniform flow conditions.

### *4.3.2 Shear Stress Contours*

Most of hydraulic formulae assume that the boundary shear stress distribution is uniform over the wetted perimeter. However it is established that such forces even in straight prismatic channel with simple cross-sectional geometry are not uniform. For meandering channel the distribution in shear stress widely varies from point to point along the wetted perimeter. Therefore, a study has been carried out to investigate the distribution of local shear stress along the channel boundary. Boundary shear stress measurements at the bend apex of a meander path covering a number of points in the wetted perimeter have been obtained from Patel's formulae for only in bank flows.

#### *4.3.2 (a) Simple meander channel*

Boundary shear force is a turbulent quantity composed of a fluctuating component superimposed on the mean value. The non-uniformity in shear stress is mostly due to this fluctuating component which is interpreted as secondary currents and is generated due to the anisotropy between the vertical and transverse turbulent intensities (Gessner, 1973). Even in straight prismatic channel with simple cross-sectional geometry the distribution of shear stress is not uniform. The interdependency of boundary shear stress and secondary flow has been recognized since long; as such it becomes difficult to understand either phenomenon without recourse to the other. Also the local shear stress largely depends on the velocity gradient near to the boundary and consequently on the pattern of isovels. Boundary shear stress distributions

along with local shear stress contours are obtained for four different depths of flow at bend apex section of the meander path and are shown in Fig.4.3 (a, b, c and d).

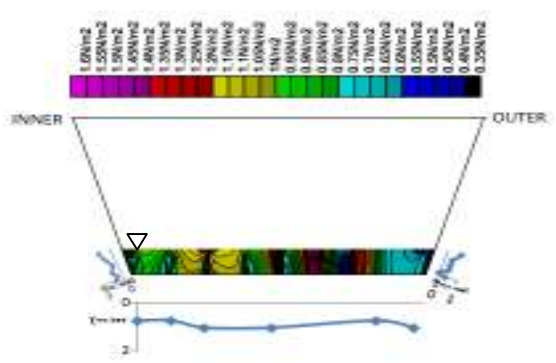


**Fig. 4.3(a) Flow Depth (*h*) = 1.7 cm**

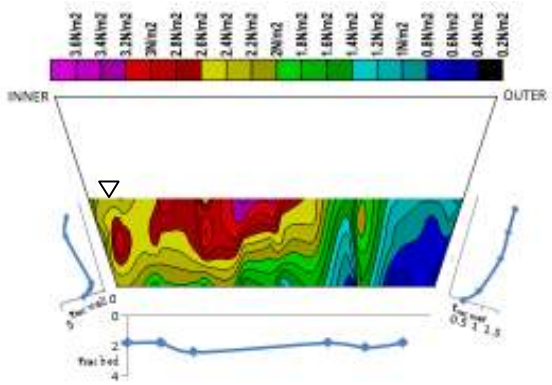


**Fig. 4.3(b) Flow depth *(h)* = 3.8 cm**

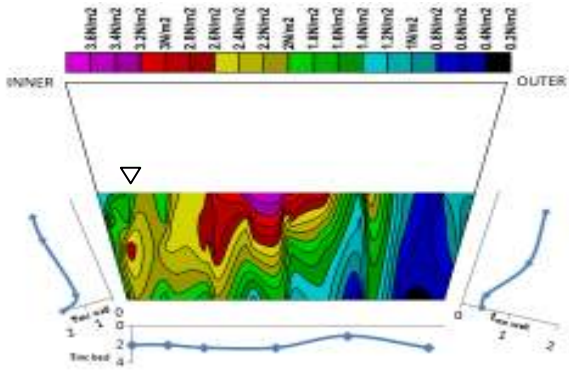


**Fig. 4.3(c) Flow depth (*h*) = 4 cm**

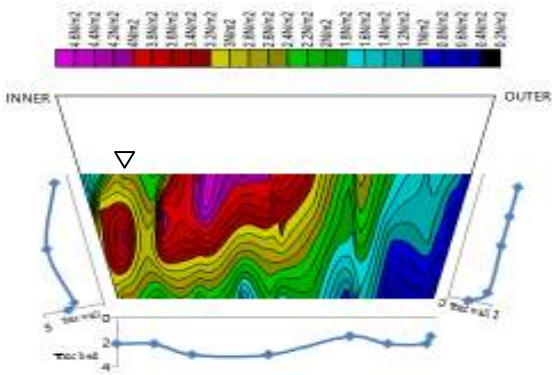


**Fig. 4.3(d) Flow depth (*h*) = 5cm**

**Fig.4.3 (a) - Fig.4.3 (d) Contours showing the local shear stresses for in bank flow at the bend apex and graph showing distribution of boundary shear stress.**

**(Longitudinal shear stress contours are in N/m$^2$)**

From the above shear stress contours the following inferences can be made:

i. The location of thread of maximum local shear stress is found to occur near the inner wall than outer wall.

ii. The distribution of boundary shear stress along the wetted perimeter in meandering channels follows sinusoidal (non-uniform) pattern. The distributons of boundary shear stress are used to highlight secondary flow currents, as the boundary stress is usually a better indicator of their presence than isovel patterns (Knight and Patel, 1985).

iii. A remarkable feature of all the distribution is that a high value of shear stress persists near the air-water interface. This is likely to happen as in these regions the surface velocities are quite large.

### *4.3.2 (b) Compound meander channel*

Fig.4.2(b) shows the grid points where the local shear stress measurements are made and the shear stress contours for four relative depths are derived which are depicted in Fig.4.4 (a)-4.4 (b).

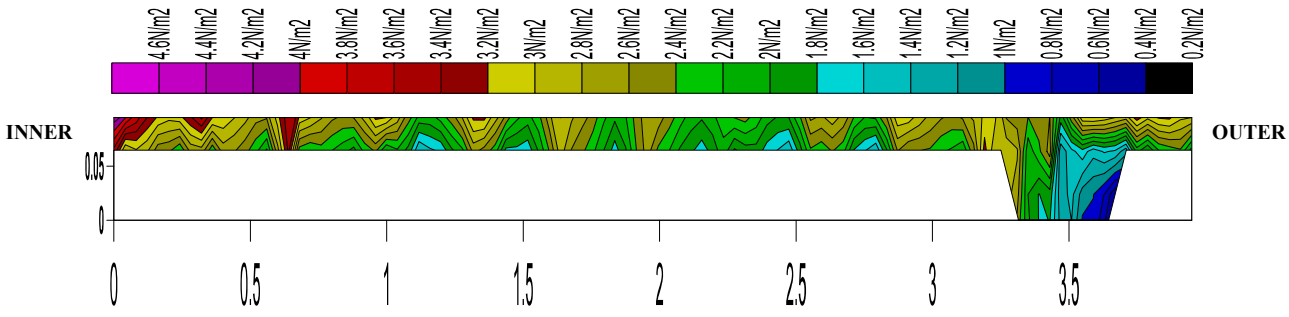


**Fig.4.4 (a) Depth of flow, ($H'$ -$h$) = 3.0 cm; $H$ = 9.5cm**

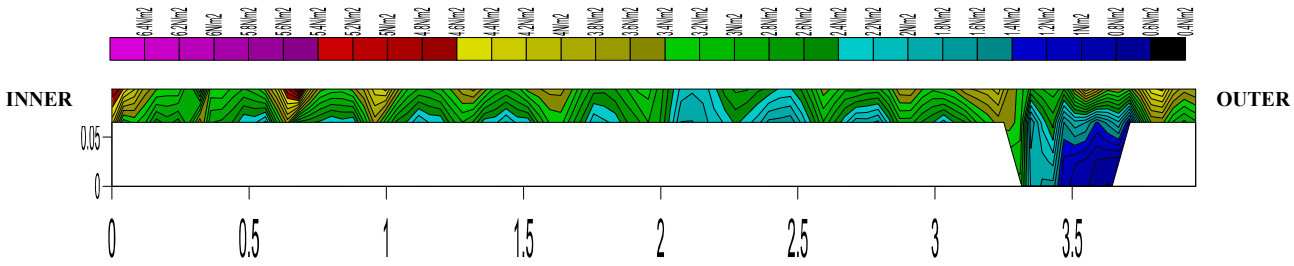


**Fig.4.4 (b) Depth of flow, ($H'$ -$h$) = 3.4 cm; $H$ = 9.9cm**

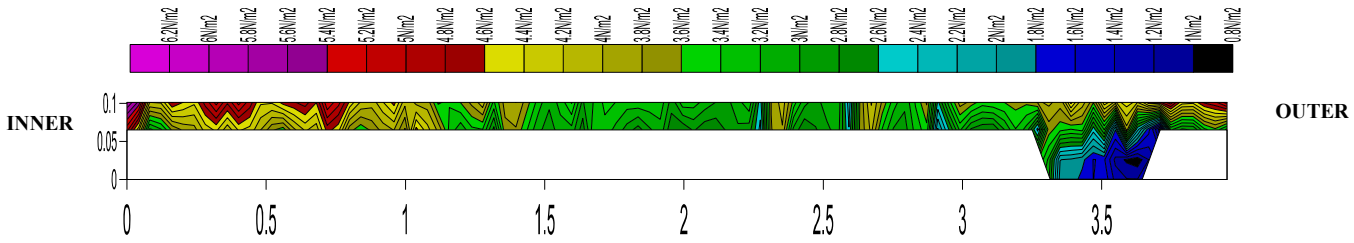


**Fig.4.4(c) Depth of flow, ($H'$ -$h$) = 3.6 cm; $H$ = 10.1cm**

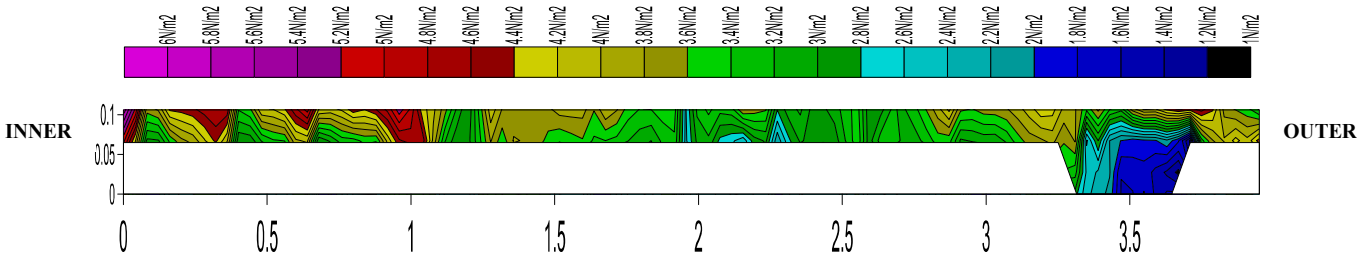


**Fig.4.4 (d) Depth of flow = ($H'$ - $h$) = 4.1 cm; $H$ = 10.6cm**

**Fig.4.4 (a) - Fig.4.4 (d) Contours showing the local shear stresses for over bank flow at the bend apex. (Longitudinal shear stress contours are in N/m$^2$)**

From the above local shear stress contours of compound meander channel for different flow depths, the following remarkable features can be noted:

i. The pattern of overbank shear stress contours is somewhat similar to that of in bank shear contours.

ii. The lowest shear stress contour lines prevail at outer main channel bottom corner and its concentration increases with the increase in flow depth over the flood plain.

iii. Another feature which is discernible from the contour diagram is that the maximum value of local shear stress occurs at inner floodplain wall and its concentration increases as the flow depth over the floodplain increases.

iv. Interestingly the local average shear stress appears more prominent in the left floodplain region.

## 4.4 ANALYSIS

### 4.4.1 MEAN BOUNDARY SHEAR STRESS

River scientists have found that water in reality does not move as an ideal frictionless fluid. Water during its motion is resisted by various forces and in doing so it consumes energy. Understanding this variation in resisting forces is of primary importance in shear studies. Water is impelled downstream by force of gravity. This force so developed in flow direction is resisted by reaction from channel boundary. If the flow is uniform, velocity does not change downstream and one may conclude from Newton's first law of motion that the driving and resisting forces must be in balance.

The relevant forces are,

Driving force ($W_s$) = downward component of the total weight of water,

$$W_s = W\,Sin\theta = \rho g A L\,Sin\theta \quad (9)$$

Resisting Force ($F_0$) = boundary shear stress* bed area,

$$F_0 = \tau_0 PL \quad (10)$$

$$\text{Now } W_s = F_0, \quad \rho g A L\,Sin\theta = \tau_0 PL \quad (11)$$

$$\tau_0 = \rho g (A/P)\,Sin\theta \quad (12)$$

The ratio ($A/P$) is known as hydraulic radius, $R_h$ (m). Substituting ($A/P$) as $R_h$ and $Sin\theta$ as slope $S$ in equation (12) we get,

$$\tau_0 = \rho g\, R_h S = \gamma R_h S \quad (13)$$

$\tau_0$ is referred as overall mean boundary shear stress or 'depth-slope product' because hydraulic radius normally is approximated by the mean depth (h) of the channel. Equation (13) denotes the variation of shear stress within the section. Furthermore this equation is strictly valid only for uniform flow. Also $\tau_0$ to some extent applies reasonably well to gradually varied flow as in experimental channel in which, at least for short reaches of channel, the flow approximates uniform conditions.

### 4.4.2 DISTRIBUTION OF BOUNDARY SHEAR STRESS

#### *4.4.2 (a) Simple meander channel*

The wall and bed shear stresses are normalized with their mean values. The variation of normalized inner and outer wall with z/H and the variation of normalized inner and outer bed shear stress with 2y/B for two types of aspect ratio are shown in Fig.4.3 and Fig.4.4 respectively. The influence of secondary currents on the boundary shear stress distribution in meandering

channel may be established from Figs.4.5 and 4.6. With reference to Fig.4.6, for lower aspect ratio (*B/H*=6.6) the maximum bed shear stress is displaced from centerline line towards a corner; whereas at higher aspect ratio (*B/H*=19.4) the maximum bed shear stress returns to the bed centerline position for inner bed region. For outer bed region the maximum bed shear stress occurs at the centerline position irrespective of the aspect ratio. Similarly the maximum value of inner and outer wall shear stress does not occur at the free surface (*z/H*=1) but at some intermediate position between the free surface and the bed (Fig.4.5).The wall and bed shear distributions exhibit certain perturbations which may be explained in terms of the number and distribution of secondary flow cells within the cross section (Knight *et.al.,* 1984). As seen from Fig.4.5, the maximum wall shear stress is positioned next to the free surface (i.e., at 0.8 depth) for low depth flow whereas for high depth flow the maximum wall shear stress occurs towards bed (i.e., at 0.08-0.4depth).

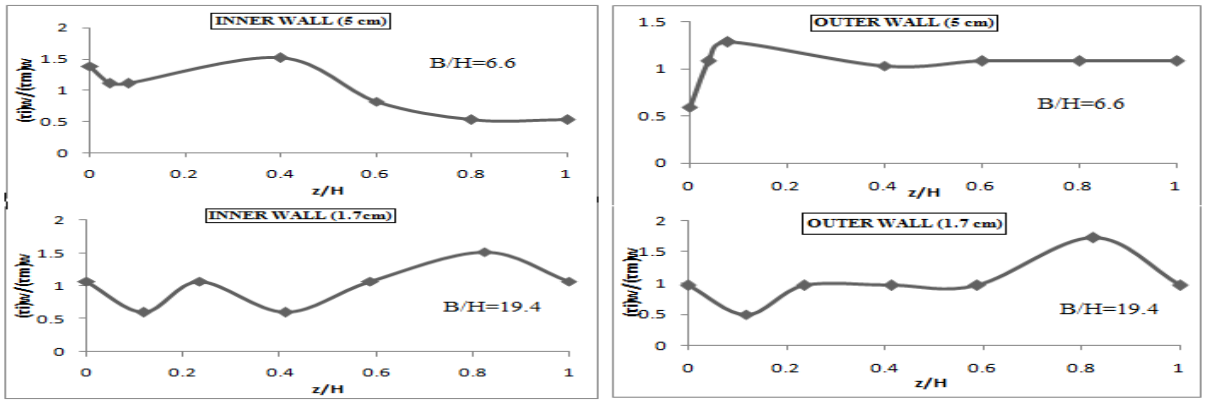


**Fig.4.5 Dimensionless local wall shear stress versus z/H for flow depths 5cm and 1.7 cm at inner and outer wall**

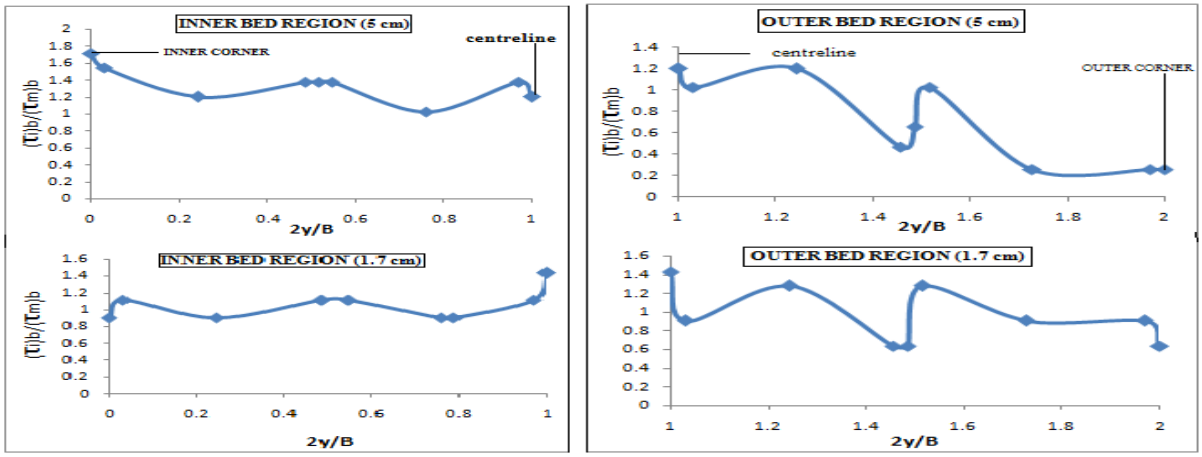


**Fig.4.6 Dimensionless local bed shear stress versus 2y/B for flow depths 5cm and 1.7 cm in inner and outer bed region**

### *4.4.2 (b) Compound meander channel*

Overbank flow cases are complicated processes to model due to the presence of turbulent structures ranging from large to small scales which transfers momentum from faster moving fluids in main channel to relatively slower fluid in flood plain while increasing and decreasing the conveyance respectively. Therefore a lot of experimental and numerical approaches has been recently adopted to quantify this lateral momentum transfer at the main channel and flood plain interface. This accretion in technical knowledge compel operating authorities should use recent improved knowledge on conveyance to reduce uncertainty in flood predictions. Taking this into account a team of experts led by HR Wallingford introduced a new Conveyance Estimation System (CES) which is being adopted in England, Wales, Scotland and Northern Ireland. CES has been recommended for use in natural rivers, artificial straight and meandering channels for estimating conveyance, computing stage discharge relationship and also a number of flow parameters like depth averaged velocity, boundary shear, shear velocity,

energy coefficients etc. The software includes a roughness advisor, conveyance generator, and an uncertainty estimator. The conveyance generator is based on 1D Shiono and Knight conveyance estimation method (SKM). Previously conveyance estimation methods incorporate only roughness parameter such as Manning's *n*, Chezy's *C* and Darcy Weisbach *f,* but SKM consists three calibration constants: Weisbach *f,* dimensionless eddy viscosity λ, transverse gradient of secondary flow term Γ. Therefore it precisely models the flow to reduce uncertainties in the estimation of river flood levels, discharge and velocities.

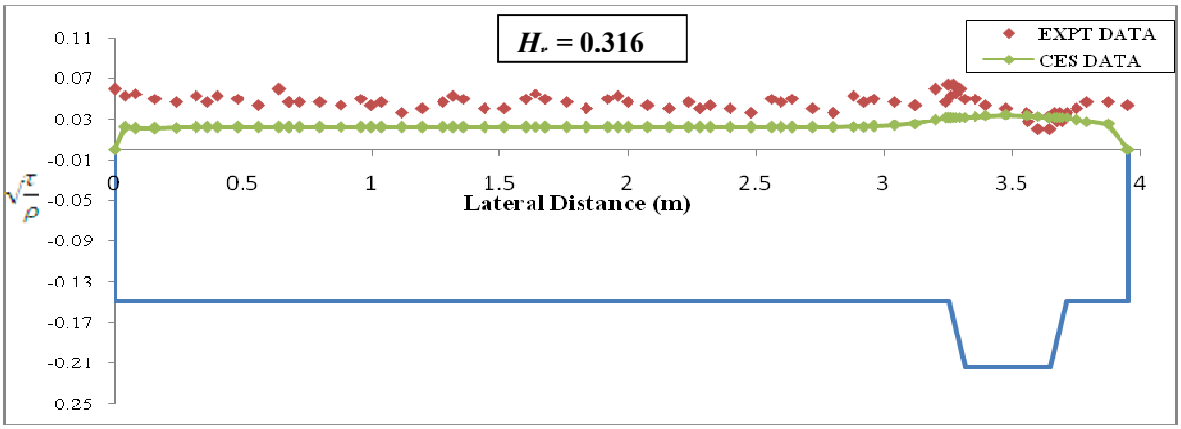


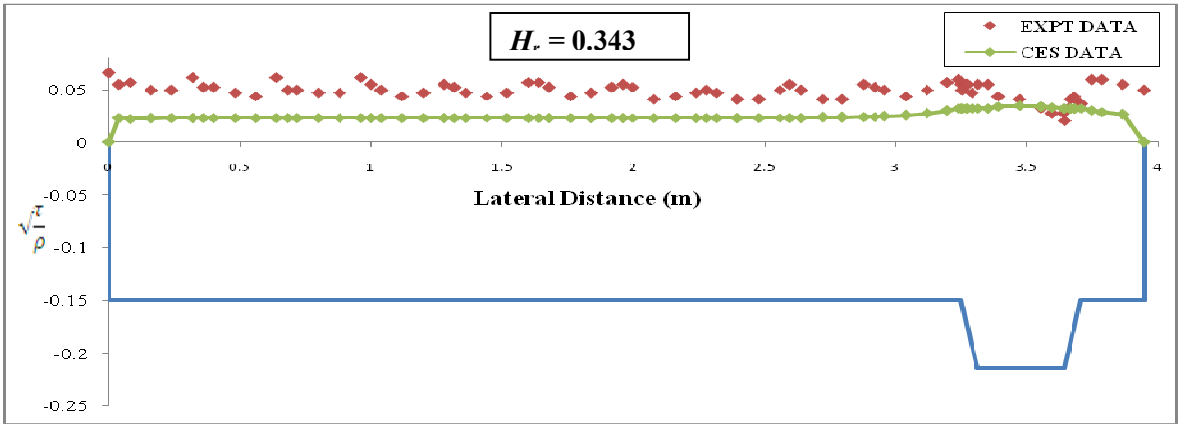

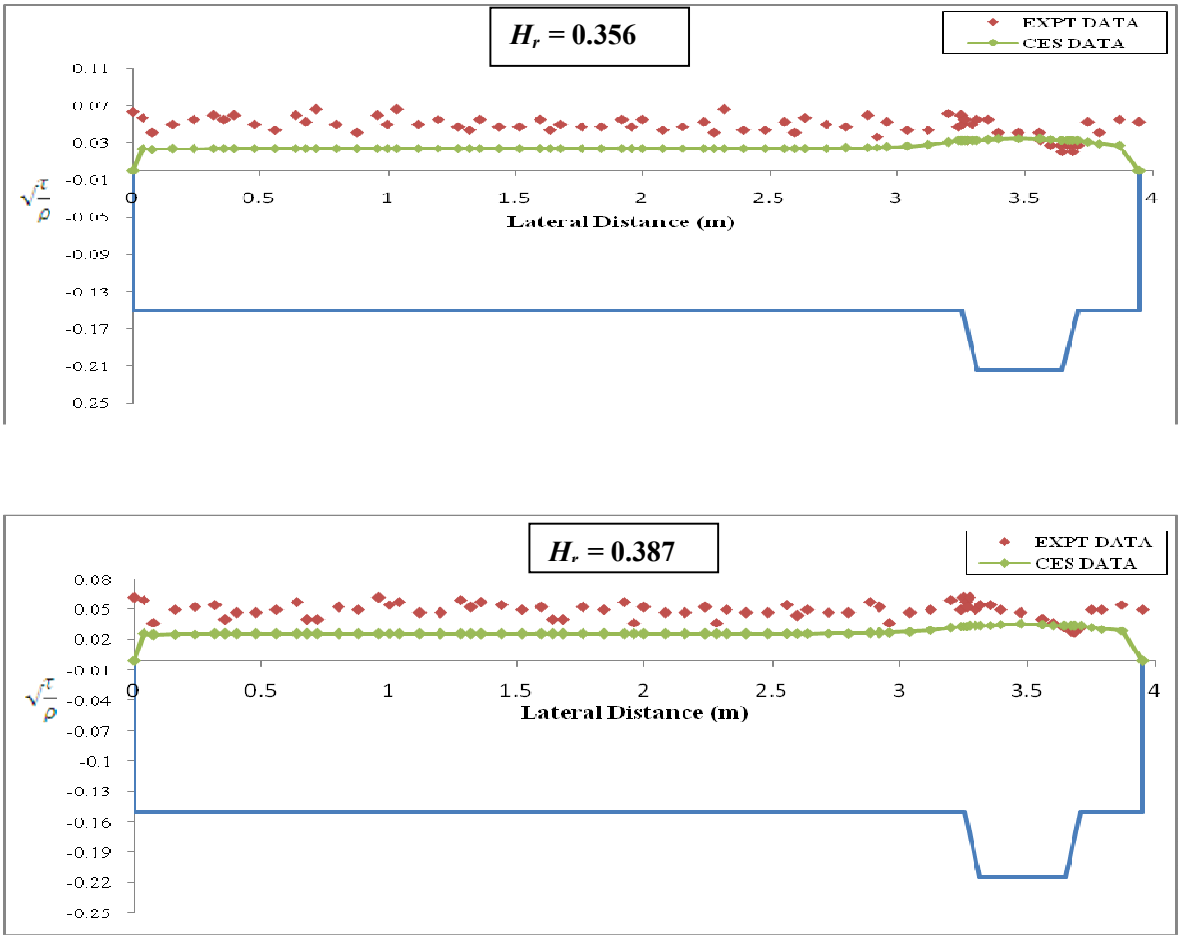


**Fig.4.7 Lateral distribution of shear velocity along the compound cross section of experimental channel at bend apex for different relative depths**

The boundary shear stress values are expressed in terms of shear velocity for different relative depths and are validated with one-dimensional modeling software conveyance estimation system (CES) which is shown in Fig. 4.7. Series 1shows the experimental values and series 2 shows the values yielded through CES. Some important inferences can be drawn from these diagrams which are summarized below:

i. In case of the present compound meandering channel, the maximum value of boundary shear stress occurred at the junction between inner main channel bank and the flood plain. However the boundary shear stress decreases in the main channel but again rises at the junction between outer main channel bank and the flood plain. But this time the increment in boundary shear stress is less as compared to the increase at the inner main channel bank and the flood plain junction.

ii. The minimum boundary shear stress occurs towards the outer bank region in the main channel.

iii. This trend of distribution of boundary shear stress gives enough indication of presence of secondary flow at main channel corner and main channel-flood plain interaction regions which is substantially affected by the large amount of momentum transportation between the main channel and flood plain (Jing *et. al.,* 2009).

iv. The quasi-1D model conveyance estimation system (CES) underestimates boundary shear stress values whereas it successfully reproduces velocity values.

### 4.4.3 SHEAR FORCE ANALYSIS

The measured local shear stresses are integrated over the respective wetted perimeter to obtain boundary shear force per unit length of the channel. The energy gradient states that the weight of water in the direction of flow in the channel is equal to the resistance offered from the channel boundary.

Shear Force per unit length of wetted perimeter, (By Energy Gradient) $F = \rho gAS$

For the experimental channels, the mean shear found from the Preston- tube agrees well with the mean value computed from energy gradient approach. The shear forces calculated from measured shear stresses along the channel boundary are tabulated below in Table 3.

**Table 3. Summary of boundary shear force results for the experimental simple meandering channels observed at bend apex.**

| Expt. Runs | Discharge ($cm^3/s$) | Average velocity (cm/s) | Flow Depth (cm) | Aspect Ratio | $SF_{bed}$ (N) | $(SF_w)_i$ (N) | $(SF_w)_o$ (N) | $SF_T$ (Actual) | $SF_T$ (Theoretical) (ρgAS) | % of error for $SF_T$ |
|---|---|---|---|---|---|---|---|---|---|---|
| M1 | 1165.29 | 19.75 | 1.7 | 19.4 | 0.300152 | 0.013155 | 0.006727 | 0.320034 | 0.318281 | 0.55 |
| M2 | 1872 | 21.09 | 2.5 | 13.2 | 0.477705 | 0.027889 | 0.019468 | 0.525061 | 0.478851 | 8.80 |
| M3 | 3803 | 27.19 | 3.8 | 8.68 | 0.665384 | 0.05687 | 0.04318 | 0.765433 | 0.754507 | 1.43 |
| M4 | 4153.37 | 28.06 | 4 | 8.25 | 0.667682 | 0.062045 | 0.038288 | 0.768014 | 0.798534 | -3.97 |
| M5 | 6055.41 | 31.87 | 5 | 6.6 | 0.779612 | 0.142777 | 0.044873 | 0.967262 | 1.025145 | -5.98 |
| M6 | 7500 | 33.33 | 5.8 | 5.69 | 0.897967 | 0.167863 | 0.065055 | 1.130886 | 1.214203 | -7.37 |

### 4.4.4 DEVELOPMENT OF MODEL

Flow and velocity distribution are more complex in meandering channels than the straight channels due to influence of continuous changing curvatures and the flow path. The flow structure becomes 3-dimensional influencing greatly to the asymmetrical nature of boundary shear distribution between inner and outer sides. This necessitates separate analysis of two banks (inner and outer) of meandering channel. Many investigators have developed empirical equations for shear force by fitting equations to the data. Knight and Hamed (1984), Knight and Patel (1985), Patra (1999) and Khatua (2008) have used the experimental data's to show the variation

of percentage of measured wall shear force to the total boundary shear force for different aspect ratios. It is ascertained that percentage of total shear force carried by walls decreases with increase in aspect ratio.

Knight *et.al* (1984) showed that for straight channel the percentage of shear in wall $SF_w$ varied exponentially with the aspect ratio [i.e., $\alpha = B/H$], that can be expressed as,

$$(\%SF_w) = e^m \qquad (14)$$

By plotting on logarithmic scale and using linear regression of $(\% SF_w)$ against $\alpha\ (= b/h)$, we can write

$$\log_{10}(\%SF_w) = 1.4026 \log_{10}\left(\frac{b}{h} + 3\right) + 3 + 2.67 \qquad (15)$$

where, $b$ is the base width and $h$ the depth of flow of water. Comparing *(1)* and *(2)* we get

$$m = 2.30259[A_1 Log_{10}\left(\frac{b}{h} + A_2\right) + A_3] \qquad (16)$$

that gives

$$m = -3.23Log_{10}(\alpha + 3) + 6.146 \qquad (17)$$

It proves that $m$ is a function of the aspect ratio [i.e. m = $f(b/h) = f(\alpha)$].

Finally, $(\%SF_w) = \exp\left(-3.23 * \log_{10}\left(\frac{b}{h} + 3\right) + 6.146\right)$ *(18)*

Khatua and Patra (2010) used two types of meandering channels with smooth and rough surfaces having sinuosity 1.21 and 1.22 for a range of aspect ratio $1.01 < \alpha < 2.45$ to further modify *(5)* to include meandering effect, given as

$$\%SF_W = e^m + 2.15S_r^{-1.06} Ln(30.692 \times \alpha) \qquad (19)$$

where $m = -3.23Log_{10}(\alpha + 3) + 6.146$

Incorporating experimental results of present study, *(6)* is now improved for higher ranges of aspect ratio $5.7 < \alpha < 19.4$ and the modified equation as follows,

$$(\%SF_w)_{mod.} = e^m + Sr^{-1.06} \ln(0.2 * \alpha - 1.1) \qquad (20)$$

where $(\%\ SF_w)_{mod.}$ = modeled percentage shear force wall of both the walls, $S_r$ = the sinuosity of meandering channel and $\alpha$ = the aspect ratio.

In addition, a non linear best fit relation between the percentage of wall shear force ($\%\ SF_w$) and the channel aspect ratio ($\alpha$) in Fig.4.8 takes the following form,

$$y = 118x^{-0.97} \qquad (21)$$

where $x$ = aspect ratio and $y = (\%\ SF_w)_{mod.}$

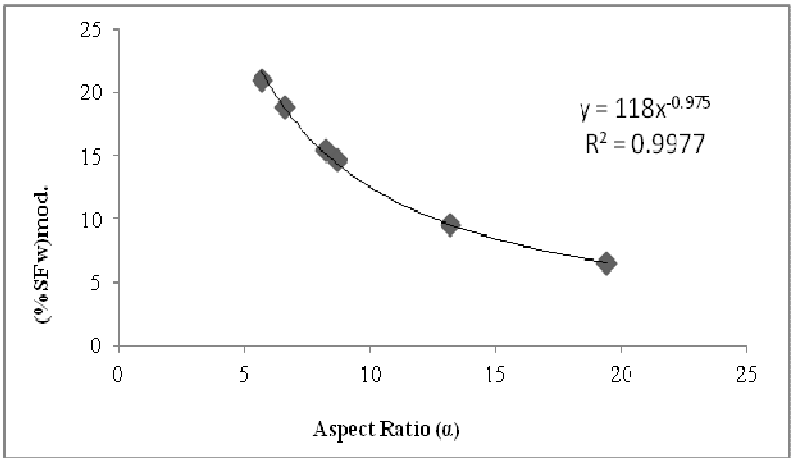


**Fig.4.8 Variation of $(\%SF_w)_{mod}$ with Aspect Ratio**

Since one of the objective of present study is to analyze inner and outer wall shear separately, the computed inner wall shear force $(SF_w)_{inner}$ and outer wall shear force $(SF_w)_{outer}$ is non-dimensionalised with total shear force to get $(\%SF_w)_{inner}$ and $(\%SF_w)_{outer}$ respectively. Variation of $(\%SF_w)_{inner}$ and $(\%SF_w)_{outer}$ with aspect ratios are shown in Fig.4.9(a) and Fig.4.9(b) respectively.

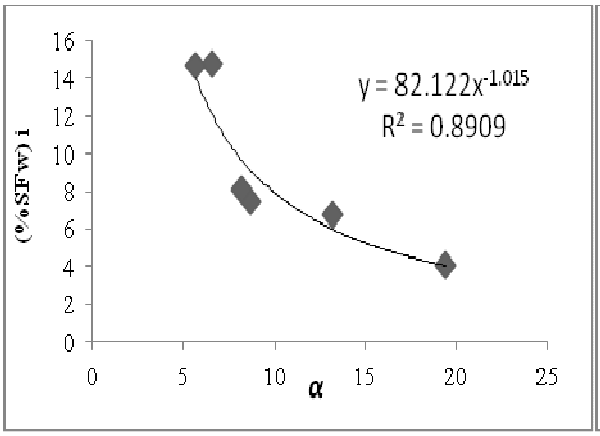


**Fig.4.9 (a) Variation of $(\%SF_w)_i$ with Aspect Ratio**

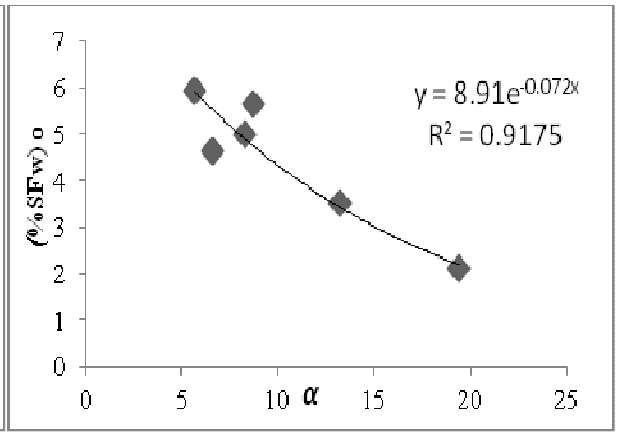


**Fig.4.9 (b) Variation of $(\%SF_w)_o$ with Aspect Ratio**

Comparing Figs.4.9 (a) and 4.9 (b), it is clear that the percentage of shear force at the inner wall is more than that of the outer wall. Usually it is found that the average shear force at inner wall is 1.3 times the average shear force at the outer wall at low in bank flows whereas the average shear force at inner walls increases by 3 folds than outer wall for higher flow depths. Also, the variation of ($\% SF_{bed}$) with aspect ratio for the observed values is shown in Fig.4.10. It is surprisingly found that, for low in bank flows average shear force at bed is 15 times higher than that of average shear force at wall whereas at higher depths the variation of shear force decreases to 4. The experimental measurements of bed shear force reveals the dominating influence of bed than wall in meandering channels at higher aspect ratio. The values of percentage shear force at the bed, at inner and outer wall has been provided in Table 4.

**Table 4. Summary of percentage shear force results along the wetted perimeter for the experimental simple meandering channels observed at bend apex.**

| Aspect Ratio (B/H) | Actual Percentage shear force on walls $(\%SF_w)_{act.}$ | Modeled Percentage shear force on walls $(\%SF_w)_{mod.}$ | Percentage shear force at inner wall $(\%SF_w)_{inner}$ | Percentage shear force at outer wall $(\%SF_w)_{outer}$ | Percentage shear force on bed $(\%SF_b)$ |
|---|---|---|---|---|---|
| 19.4 | 6.212461 | 6.43401 | 4.110434 | 2.101953 | 93.78761 |
| 13.2 | 10.13039 | 9.589239 | 6.757115 | 3.51718 | 92.55157 |
| 8.68 | 13.07096 | 14.63293 | 7.429735 | 5.641221 | 86.92904 |
| 8.25 | 13.06392 | 15.37401 | 8.078583 | 4.985335 | 86.93608 |
| 6.6 | 19.40013 | 18.8445 | 14.761 | 4.639132 | 80.59987 |
| 5.69 | 19.70742 | 20.95215 | 14.69801 | 5.949956 | 79.54673 |

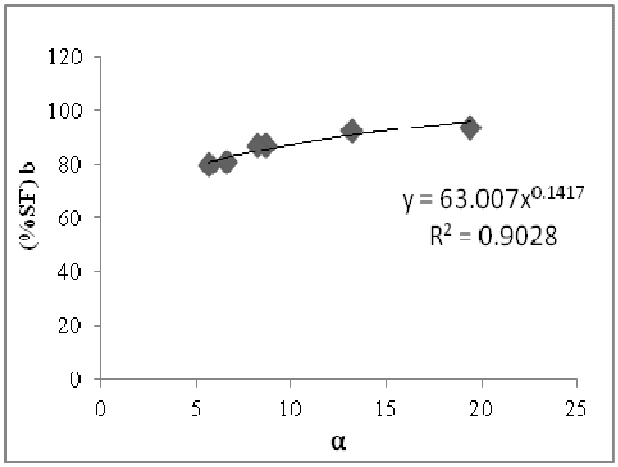


**Fig.4.10 Variation of (*%SF $_{bed}$*) with Aspect Ratio**

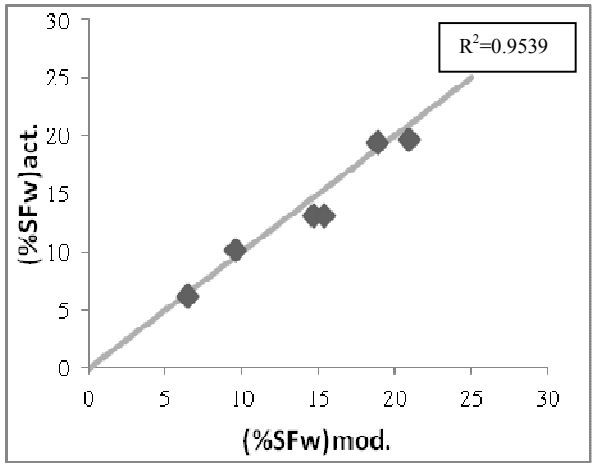


**Fig.4.11 Observed and modeled values of (*%SF$_w$*)**

The variation of error in the computation of (*%SF$_w$*) by the proposed *(20)* against observed (*%SF$_w$*) is plotted in Fig.4.11 giving the least error which shows adequacy of developed equation.

# NUMERICAL MOELING

## 5.1 GENERAL

Computational Fluid Dynamics (CFD), is a branch of fluid mechanics that uses numerical methods and algorithms to solve and analyze problems that involve fluid flows. Computers are used to perform the calculations required to simulate the interaction of liquids and gases with surfaces defined by boundary conditions. With high-speed supercomputers, better solutions can be achieved. Ongoing research yields software that improves the accuracy and speed of complex simulation scenarios such as transonic or turbulent flows. It has started around 1960 and with the process of improvement in computer processor speed, CFD simulation is now showing astounding accuracy. The CFD based simulation relies on combined numerical accuracy, modeling precision and computational cost.

The fundamental basis of almost all CFD problems is the Navier–Stokes equations, which define any single-phase fluid flow. These equations can be simplified by removing terms describing viscosity to yield the Euler equations. Further simplification, by removing terms describing vorticity yields the full potential equations. Finally, for small perturbations in subsonic and supersonic flows these equations can be linearized to yield the linearized potential equations. There is no direct solution of the equation for flow. The N-S in vector form for single phase incompressible fluid flow can be expressed as:

$$\frac{\partial}{\partial t}(\rho \bar{u}_i) + \frac{\partial(\rho \bar{u}_i \bar{u}_j)}{\partial z_i} = \frac{\partial}{\partial z_j}\left(\mu \frac{\partial \sigma_{ij}}{\partial z_j}\right) - \frac{\partial \bar{p}}{\partial z_i} - \frac{\partial \tau_{ij}}{\partial z_j} \qquad (22)$$

Where $\sigma_{ij}$ and $\tau_{ij}$ are normal and shear stress component on any assumed plane normal to i along j direction. $\bar{u}_i'$, $\bar{u}_j'$ are time averaged instantaneous velocity component along i,j

directions. $p$ = pressure, μ = co-efficient of viscosity, $\rho$ = density. The process of the numerical simulation of fluid flow using the above equation generally involves four steps and the details are:

(a)Problem identification

1. Defining the modeling goals
2. Identifying the domain to model

(b) Pre-Processing

1. Creating a solid model to represent the domain (Geometry Setup)
2. Design and create the mesh (grid)
3. Set up the physics
    - Defining the condition of flow (e.g turbulent, laminar etc.)
    - Specification of appropriate boundary condition and temporal condition.

(c) Solver

1. Using different numerical schemes to discretize the governing equations.
2. Controlling the convergence by iterating the equation till accuracy is achieved

(d) Post processing

1. Visualising and examining the results
2. Considering revisions to the model

## 5.2 GEOMETRY SETUP

The fluid flow governing equations (momentum equation, continuity equation) are solved based on the discretization of domain using the Cartesian co-ordinate system. This procedure involves

dividing the continuum into finite number of nodes. The CFD computations need a spatial discretization scheme and time marching scheme. Mainly the domain discretization is based on Finite element, Finite Volume and Finite Difference Method. Finite Element method is based on dividing the domain into elements. The numerical solution can be obtained in this method by integrating the shape function and weighted factor in an appropriate domain. This method is suitable with respect to both structured and unstructured mesh. The application of Finite Volume method needs dividing the domain into finite number of volumes. Here the specified variables are calculated by solving the discreitized equation in the centre of the cell. This method is developed by taking conservation law in to account. Finite Volume method is suitable for applying in unstructured domain. Finite Difference method is based on Taylor's series approximation. This method is more suitable for regular domain.

The meandering open channel corresponding to one wavelength of five wavelengths is continuously constructed in the experimental flume. In the experimental flume, five meander waves are fabricated for the case of $S_r$ = 1.29, where the sinuosity, $S_r$, is defined as the ratio of the meandering channel length to the meander wavelength. One meander wavelength has trapezoidal cross-section with following dimensions: bed width, 330mm; top width, 460mm; main channel depth, 65mm; meander wavelength, 4170 mm and central angle of the bend; 120°. Each section has a 60° circular bend with the centreline radius of 1.1 m followed by a 0.68m straight reach which approximates a sine generated meandering curve. For the present case of numerical solution, the flow is simulated at 50 mm depth of water in the meander channel.

## 5.3 DISCRETIZATON OF DOMAIN (MESHING)

The discretization of complex computational domain is critical. These kinds of domain don‘t coincide with the co-ordinate lines with that of a structured grid, which leads to approximation of the geometry. The only procedure to represent complex computational domain is to use a stepwise approximation. But such an approximation is also arduous and quite time consuming. Further, the stepwise approximation introduces truncation error and that can be overcome by providing very fine Cartesian mesh. In whichever way the domain is discretised, based on mesh methods such as any of those mentioned above, care has to be taken in order to produce a good mesh. A mesh with too few nodes could lead to a quick solution, yet not a very accurate one. However a very dense mesh of nodes will potentially waste computational time and memory. Usually more nodes are required within areas of interest, such as near wall and wake regions, in order to capture the large variation of fluid properties expected in these regions. Thus, structure of grid lines causes further wastage of computer storage due to un-necessary refinement. In this study, the flow domain is discretized using structured grid and body-fitted coordinates. The detailed meshing of the flow domain with two views is shown in Fig.5.1

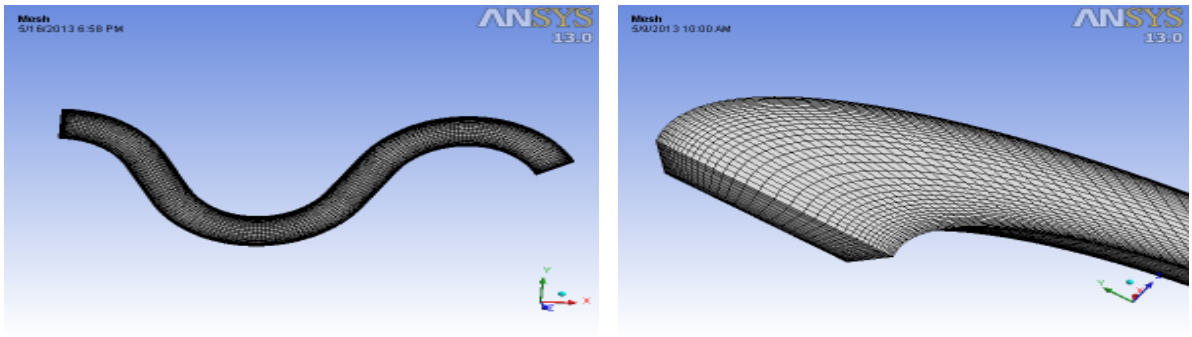


**Fig. 5.1 Schematic diagram of structured mesh**

## 5.4 TURBULENCE

Turbulent flow is a flow regime characterized by chaotic and stochastic property changes. This includes low momentum diffusion, high momentum convection, and rapid variation of pressure and velocity in space and time. Turbulence occurs when the inertia forces in the fluid become significant compared to viscous forces, and is characterized by a high Reynolds Number. In principle, the Navier-Stokes equations describe both laminar and turbulent flows without the need for additional information. However, turbulent flows at realistic Reynolds numbers span a large range of turbulent length and time scales, and would generally involve length scales much smaller than the smallest finite volume mesh, which can be practically used in a numerical analysis. The Direct Numerical Simulation (DNS) of these flows would require computing power which is many orders of magnitude higher than available in the foreseeable future. To enable the effects of turbulence to be predicted, a large amount of CFD research has concentrated on methods which make use of turbulence models. Turbulence models have been specifically developed to account for the effects of turbulence without recourse to a prohibitively fine mesh and direct numerical simulation. Most turbulence models are statistical turbulence model, as mentioned below.

**Turbulence Models**

- Algebraic (zero-equation) model
- k-ε, RNG k-ε
- Shear stress transport
- k-ω

- Reynolds stress transport model (second moment closure)
- k-ω Reynolds stress
- Detached eddy simulation (DES) turbulence model
- SST scale adaptive simulation (SAS) turbulence model
- Smagorinsky large eddy simulation model (LES)
- Scalable wall functions
- Automatic near-wall treatment including integration to the wall
- User-defined turbulent wall functions and heat transfer

The two exceptions to this in ANSYS CFX are:

• Large Eddy Simulation Theory

• Detached Eddy Simulation Theory

However open-channel flows are characterized by complicated flow structures, even for simple geometry, such as that of a rectangular channel. This is largely due to wall and free surface boundaries. The secondary currents are generated in open channel flows because free surface and walls reduce the turbulence intensity in the direction normal to the surface or the walls and lead to anisotropy of turbulence. The three dimensional nature of turbulent flow can be decomposed into mean part and fluctuation part, which is called Reynolds decomposition. Gravity and channel geometry are mainly responsible for turbulent flow for this particular condition.

## 5.5 NUMERICAL MODEL

### *5.5.1 Large Eddy Simulation (LES)*

The three major types of turbulence methodologies are Direct Numerical Simulation (DNS), Large eddy Simulation (LES) and k-epsilon modelling. k-epsilon models the turbulent flows by

time or space averaging. But it is not suitable for transient flows because the averaging process removes most of the important characteristics of a time-dependent solution. On the other hand, Direct Numerical Simulation, attempts to solve all time and spatial scales. As a result, the solution is very accurate. However to resolve almost all ranges of scales, the spatial and temporal grids would need to be extremely small in the order of Kolmogorov length and time scale, resulting in a problem which would take an extraordinarily long time to solve, making it computationally intensive.

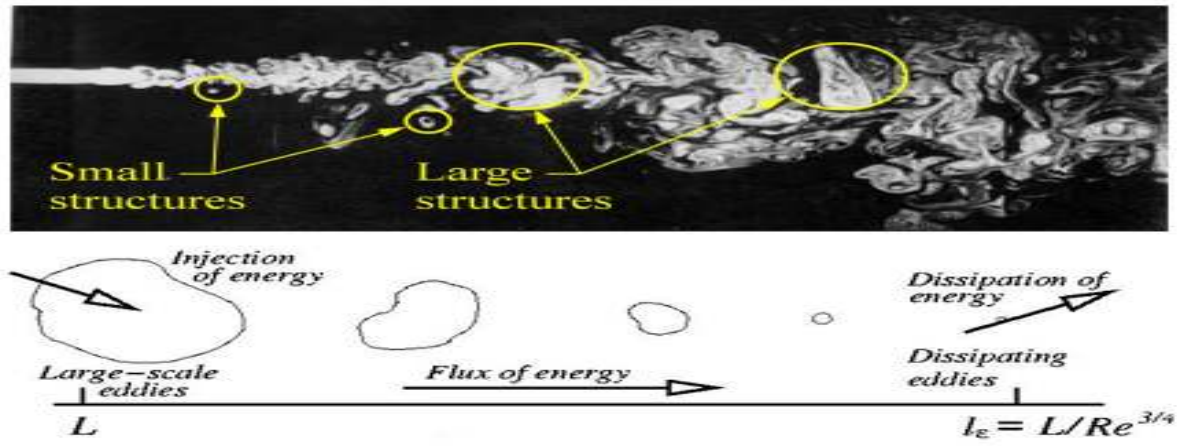


**Fig. 5.2 Energy cascade process with length scale**

One compromise between these two models is Large Eddy Simulation. Large Eddy Simulation directly solves large spatial scales (DNS), while modeling the smaller scales (k-epsilon). First, the larger scales that carries the majority of the energy, which accounts for 80% of turbulent flow energy and hence is more important. Second, the smaller scales have been found to be more universal, and hence are more easily modeled. The resulting methodology is a hybrid between these two methods, which involves the filtering of the Navier-Stokes equations to separate those

scales which will be modeled from those which will be solved for directly. Subsequently LES method simulates large scale turbulent motions directly, while the unresolved small scale motions are modeled through the use of a Smagorinsky model. This model captures larger scale motion such as DNS, as well as it covers the effects of small scales of eddies by using sub-grid scale (SGS) model.

### *5.5.2 Mathematical Model*

Large Eddy Simulation (LES) is about filtering of the equations of movement and decomposition of the flow variables into a large scale (resolved) and a small scale (unresolved) parts. Any flow variable *f* can be written such as:

$$f = \overline{f} + f' \tag{23}$$

Where $\overline{f}$ the large scale part, is defined through volume averaging as:

$$\overline{f}(x_i, t) = \int_{Vol} G(x_i - x_i') f(x_i', t) dx_i'$$

Where, $G(x - x')$ is the filter function (called the hat filter or Gaussian filter). After performing the volume averaging and neglecting density fluctuations, the filtered Navier-Stokes equations become:

$$\frac{\partial(\rho \overline{U_i})}{\partial t} + \frac{\partial(\rho \overline{U_i U_j})}{\partial x_j} = -\frac{\partial \overline{p}}{\partial x_i} + \mu \frac{\partial^2 \overline{U_i}}{\partial x_j \partial x_j} \tag{24}$$

The non linear transport term in the filtered equation can be developed as:

$$\overline{U_i U_j} = \overline{(\overline{U_i} + u_i')(\overline{U_j} + u_j')} = \overline{\overline{U_i}\,\overline{U_j}} + \overline{\overline{U_i} u_j'} + \overline{\overline{U_j} u_i'} + \overline{u_i' u_j'}$$

(1) (2) (3) (4)

In time, averaging the terms (2) and (3) vanish, but when using volume averaging, this is no longer true.

Introducing the sub-grid scale (SGS) stresses, $\tau_{ij}$, as:

$$\tau_{ij} = \overline{u_i u_j} - \overline{U}_i \overline{U}_j \qquad (25)$$

we can rewrite the filtered Navier-Stokes equations as:

$$\frac{\partial(\rho \overline{U}_i)}{\partial t} + \frac{\partial(\rho \tau_{ij} + \rho \overline{U}_i \overline{U}_j)}{\partial x_j} = -\frac{\partial \bar{p}}{\partial x_i} + \mu \frac{\partial^2 \overline{U}_i}{\partial x_j \partial x_j}$$

$$\frac{\partial(\rho \overline{U}_i)}{\partial t} + \frac{\partial(\rho \overline{U}_i \overline{U}_j)}{\partial x_j} = -\frac{\partial \bar{p}}{\partial x_i} + \mu \frac{\partial^2 \overline{U}_i}{\partial x_j \partial x_j} - \frac{\partial(\rho \tau_{ij})}{\partial x_j} \quad \text{with} \qquad (26)$$

$$\tau_{ij} = \overline{u_i u_j} - \overline{U}_i \overline{U}_j = \overline{\overline{U}_i \overline{U}_j} + \overline{\overline{U}_i u_j'} + \overline{\overline{U}_j u_i'} + \overline{u_i' u_j'} - \overline{U}_i \overline{U}_j = L_{ij} + C_{ij} + R_{ij}$$

$$C_{ij} = \overline{\overline{U}_i u_j'} + \overline{\overline{U}_j u_i'} = \text{Cross Terms}$$

Above equation is the basis of the LES technique. LES explicitly models smaller scale motions thereby reducing the computational cost to a larger extent than DNS in which effort is given in modeling smaller scales whereas larger scales predominantly contains energy and anisotropy.

**Sub-Grid Scale Models**

The non-linear transport of energy generates ever-smaller scales like a cascade process until it reaches the size of Kolmogorov scales as shown in Fig.5.2. The essence of LES is to account for this energy cascade from resolved large scales to the unresolved sub-grid scales. This is the role of the SGS model. The most popular class of SGS models is the eddy-viscosity type, based on (variants of) the Smagorinsky model (Smagorinsky, 1963).

**Smagorinsky Model**

The Smagorinsky model can be thought of as combining the Reynolds averaging assumptions given by $L_{ij} + C_{ij} = 0$ with a mixing-length based eddy viscosity model for the Reynolds SGS tensor. It is thereby assumed that the SGS stresses are proportional to the modulus of the strain rate tensor, $\bar{S}_{ij}$ of the filtered large-scale flow:

$$\tau_{ij} - \frac{1}{3}\tau_{kk} = -2 \cdot \nu_{SGS} \cdot \bar{S}_{ij} = -\nu_{SGS} \cdot \left( \frac{\partial \overline{U}_i}{\partial x_j} + \frac{\partial \overline{U}_j}{\partial x_i} \right) \qquad (27)$$

To close the equation, a model for the SGS viscosity $V_{SGS}$ is needed. Based on dimensional analysis, the SGS viscosity can be expressed as:

$$\nu_{SGS} \propto l \, q_{SGS}$$

where l is the length scale of the unresolved motion (usually the grid size $\Delta = (vol)^{1/3}$ ) and $q_{SGS}$ is the velocity of the unresolved motion. In the Smagorinsky model, based on an analogy to the Prandtl mixing length model, the velocity scale is related to the gradients of the filtered velocity:

$$q_{SGS} = \Delta |\bar{S}| \text{ where } \quad |\bar{S}| = (2\bar{S}_{ij}\bar{S}_{ij})^{1/2} \qquad (28)$$

This yields the Smagorinsky model for the SGS viscosity:

$$\nu_{SGS} = (C_S \Delta)^2 |\bar{S}| \qquad (29)$$

with $C_s$ the Smagorinsky constant. The value of the Smagorinsky constant for isotropic turbulence with inertial range spectrum:

$$E(k) = C_k \varepsilon^{2/3} k^{-5/3} \text{ is } \quad C_S = \frac{1}{\pi}\left( \frac{2}{3C_k} \right)^{3/4} = 0.18 \qquad (30)$$

For practical calculations, the value of $C_s$ is changed depending on the type of flow and mesh resolution. Its value is found to vary between a value of 0.065 (channel flows) and 0.25. Often a value of 0.1 is used.

## 5.6 BOUNDARY CONDITIONS

### *5.6.1 Wall*

A no-slip boundary condition is the most common boundary condition implemented at the wall and prescribes that the fluid next to the wall assumes the velocity at the wall, which is zero.

$U = V = W = 0$

### *5.6.2 Free Surface*

Here, Symmetry Boundary condition is used for the free-surface. This condition follows that, no flow of scalar flux occurs across the boundary. In applying this condition normal velocities are set to zero and values of all other properties outside the domain are equated to their values at the nearest node just inside the domain. Here the experimental bulk velocity of the flow is initially approximated as

$W$ = 0.319 m/s, $V = 0$, $U = 0$ and $\frac{\partial w}{\partial z} = 0$

### *5.6.3 Inlet and Outlet Boundary Condition*

To initialize the flow a mean velocity was specified over the whole inlet plane and is computed by $U_{in}=Q/A$, where $Q$ is the flow discharge of the channel and $A$ is the cross section area o f the inlet. A pressure gradient was further specified across the domain to drive the flow. In order to specify the pressure gradient the channel geometries were all created flat and the effects of gravity and channel slope implemented via a resolved gravity vector. It represents the angle between the channel slope and the horizontal, the gravity vector is resolved in x, y and z components as ($\rho g sin\theta \; 0 \; -\rho g cos\theta$).

Where $\theta$ = angle between bed surface to horizontal axis. Here, the $x$ component denotes the direction responsible for flow of water along the channel and the z component is responsible for creating the hydrostatic pressure. From the simulation, $z$ component of the gravity vector ($-\rho g cos\theta$) is found to be responsible for the convergence problem of the solver.

Opening type boundary condition is imposed at the outlet.

## 5.7 NUMERICAL RESULTS

ANSYS-CFX 13.0 solver manager is used to carry out the simulation process. Here the advection term is discretized with bounded central difference scheme and transient terms are discretized with Second order scheme. Courant number ($C_r$) is controlled between 0 - 0.5 and the transient time step size is taken as 0.001 s. After that, the equation is iterated over and over till desirable level of accuracy of $10^{-6}$ of residual value is achieved.

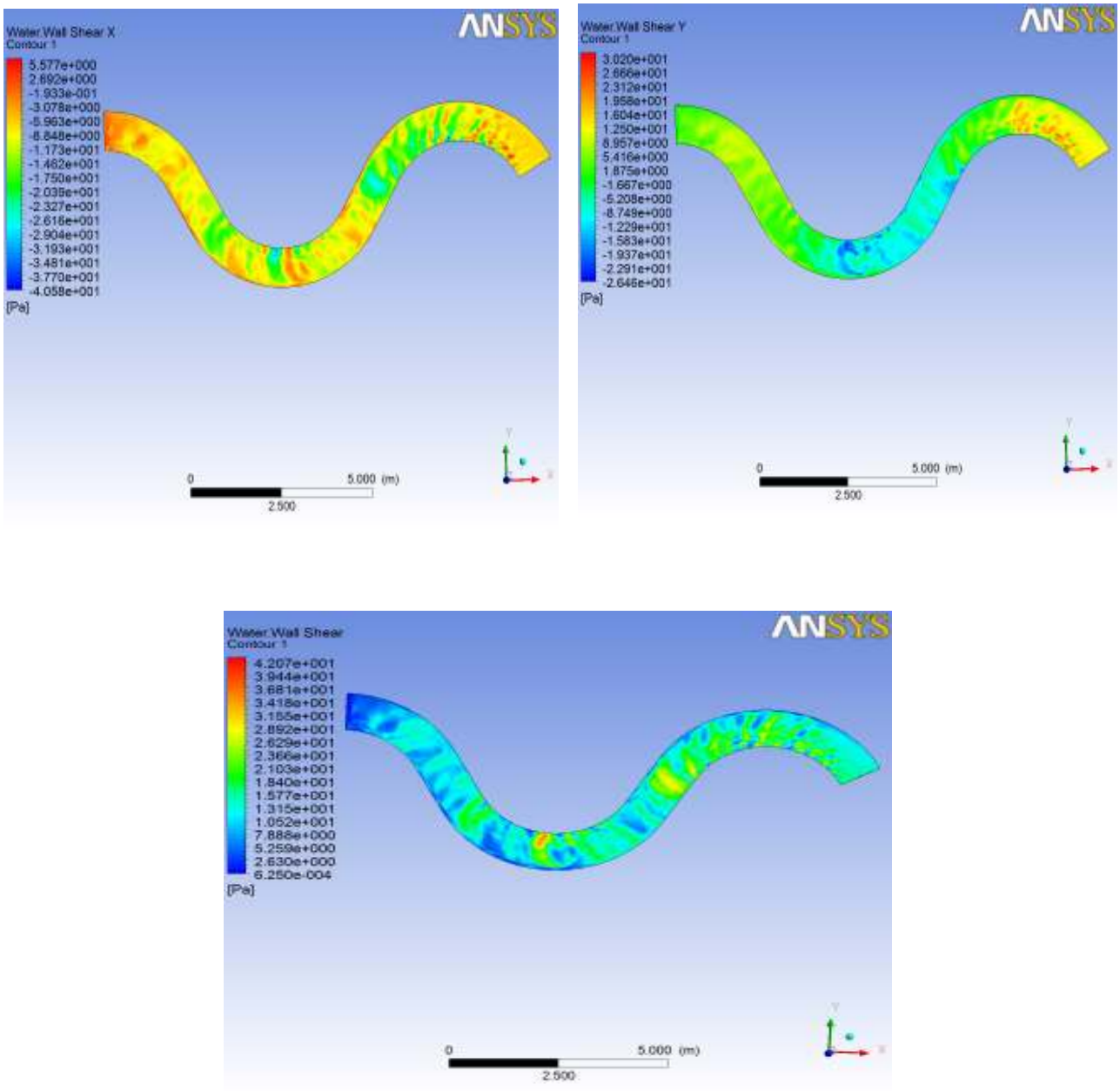


**Fig. 5.3 Contours of bed shear stress (longitudinal, lateral and resultant) along one wavelength reach of the 60° meandering channel**

One of the turbulent flow properties, bed shear stress is simulated for the 60 degree simple meandering channel. The simulation results show that the flow patterns are similar to experimental studies. Figure 5.3 shows the contours of bed shear in longitudinal, lateral and resultant directions.

Tominaga and Nezu (1991) noticed that the flow is considered to be uniform incompressible fully developed turbulent flow at a test section of 7.5 m. As it can be seen from the above figures that the flow becomes fully developed at third bend apex of the channel reach. The numerically modeled resultant bed shear stress at the third bend apex shows similar pattern of distribution as that of experimental bed shear stress. The contours of experimental shear stress as shown in Figures 4.3 (a)-4.3(d) depicts the presence of maximum thread of shear stress values towards inner bed region, as such the modeled bed shear stress reveals almost the same distribution pattern. Figure 5.3 demonstrates that the maximum resultant shear stress occurs near the inner side of the main channel as the flow enters the curved part from the straight reach. But in the straight reach region (at the point of inception) the thread of maximum shear stress gradually shifts to channel centerline. It is seen that the numerical simulation is in reasonable agreement with the experimental measurements.

# CONCLUSIONS AND FURTHER WORK

## 6.1 CONCLUSIONS

Experiments are carried out to investigate the effect of sinuosity and channel aspect ratio on the boundary shear in a meandering channel. Point to point observations are made at bend apex of meandering channel for wall shear data at different aspect ratio and for a higher sinuosity (*Sr* = 2.04) of 90° bend meander channel. Based on analysis and discussions of the experimental investigations certain conclusions from the present work are as discussed below:

- For simple meander channel, results show that shear force values are skewed and more shear force is observed at the inner wall than outer wall contrary to the findings for the narrow and deep channels.
- It is also observed in case of simple meandering channel that, as the aspect ratio in the main channel decreases the ratio of shear force between the inner and outer walls increase indicating that the shear force per unit length at inner wall increases faster with respect to the outer walls. Similarly, it can be seen that though the bed and wall shear increases with depth of flow in main channel, the rate of increase in wall shear is nearly four times the rate of increase in bed shear giving rise drastic decrease in the ratio of bed to wall shear with decrease in aspect ratio.
- The proposed *(20)* in this study can estimate wall shear forces for simple meandering channels provided channel geometry, width, flow depth and sinuosity are known. The equation is good for channels with higher aspect ratio.
- Sinusoidal distribution of boundary shear stress along the wetted perimeter is observed which confirms the presence of secondary currents in meandering in bank flows.

- Functional relationship between percentage of shear force carried by bed, inner and outer wall of meandering channel have been analysed as a function of depth ratio. Power expressions with higher correlation degrees have been obtained at the bed and inner wall whereas exponential relationship holds good at outer wall.
- Interestingly it is found that the pattern of overbank shear stress contours is somewhat similar to that of in bank shear contours. A trend of distribution of boundary shear stress has been extensively studied in compound meandering channel which gives enough indication of presence of secondary flow at main channel corner and main channel-flood plain interaction regions that is substantially affected by the large amount of momentum transportation between the main channel and flood plain.
- For compound meandering channel, the observed boundary shear stress data in terms of shear velocity is validated with CES and it is concluded that unlike velocity/depth-averaged velocity, CES underestimates shear velocity.
- Numerical analysis has been performed for the fully developed turbulent flow of a 60° simple meandering channel using Large Scale Eddy model in ANSYS CFX 13.0. The bed shear stresses results are thus derived in the form of contour which is in agreement with the experimental results.

## 6.2 RECOMMENDATIONS FOR FUTURE WORK

The present research is restricted to sole channel geometry, nature of surface and sinuosity of the meandering channel. The work thereof leaves a broad spectrum for other investigators to explore many intricate flow phenomena such as secondary currents, turbulent intensities and vortices that significantly affects the distribution of boundary shear stress in simple and compound meandering channel. Evaluation of boundary shear stress distribution has been performed for the simple and compound meandering channels involving limited data. The

equations developed may be improved by incorporating more data from channels of different geometries and sinuosity. The future scope of the present work may be summarized as:

1. Distribution of boundary shear stress components in lateral and vertical directions can be evaluated which has implications for the sediment transport studies.
2. The present work lacks shear force analysis for over bank flow conditions. The percentage of floodplain and main channel shear can be estimated and models can be developed incorporating present data.
3. The current data can be used to validate with data of other investigators and natural rivers.
4. Modeling by conventional methods is not reliable due to its instinct one dimensional modeling of flow. Though the computational methods effectively capture intricate turbulent structures in flow but require huge computer resources. Thus analytical methods based on mechanism of energy transportation, momentum and continuity equations can be solved with least approximation.
5. The channel here is smooth and rigid. Further investigation for the distribution of boundary shear stress may also be carried out for mobile beds and by roughening the channel bed.
6. LES and other turbulence closure models like k-ε, k-ω, RSM etc can be used to simulate various channel geometry with different hydraulic conditions.

# REFERENCES


1. Ansari.K., Morvan.H.P. and Hargreaves.D.M. (2011).“Numerical Investigation into Secondary Currents and Wall Shear in Trapezoidal channels.” *Journal of Hydraulic Engineering (ASCE)2011*;Vol.137 (4):432-440.
2. Beaman F.(2010). “Large Eddy Simulation of open channel flows for conveyance estimation.” Ph.D thesis, University of Nottingham.
3. Boussinesq, J. (1868). Mémoire sur l’influence des frottements dans les mouvements reguliers des fluids. J. Math. Pures Appl. (2me sér.), 13, 377-424.
4. Cater, J.E., and Williams, J.R. (2008). “Large eddy simulation of a long asymmetric compound open channel.” *Journal of Hydraulic Research.* Vol. 46(4).
5. Celik I, Rodi W. (1988). “Modeling suspended sediment transport in non-equilibrium situation.” *Journal of Hydraulic Engineering (ASCE) 1988*; 114:1157 – 1191.
6. Chiu, C. L., and Chiou, J. D. (1986). “Structure of 3-D flow in rectangular open-channels.” *J. Hydraul. Eng.,* 112(11), 1050–1068.
7. Cokljat D, Younis BA.(1995). “Second-order closure study of open channel flows.” *Journal of Hydraulic Engineering (ASCE) 1995;* 121:94 – 107.
8. Dash. S.S., Khatua. K.K and Mohanty. P.K. (2013). “Factors influencing the prediction of resistance in a meandering channel”. *International Journal of Scientific & Engineering Research* Volume 4, Issue 5, May-2013.

9. Dey S and Cheng N S (2005): "Reynolds stress in open channel flow with upward seepage". *Journal of Engineering Mechanics, American Society of Civil Engineers (ASCE),* Vol. 131, No. 4, pp. 451-467.
10. Dey S and Lambert M F (2005). "Reynolds stress and bed shear in non-uniform unsteady open channel flow". *Journal of Hydraulic Engineering, American Society of Civil Engineers (ASCE),* Vol. 131, No. 7, pp. 610-614.
11. Einstein, H. A. (1942). "Formulas for the transportation of bed-load." Trans. Am. Soc. Civ. Eng., 107, 561–597.
12. Ervine D. A., Koopaei K.B., and Sellin R. H.. J. (2000)." Two-Dimensional Solution for Straight and Meandering Over-bank Flows." *Journal of Hydraulic Engineering*, ASCE, Vol. 126, No. 9, September, paper No.22144, 653-669.
13. Ghosh, S.N., and Jena, S.B.(1971). "Boundary Shear Distribution in Open Channel Compound." Proceedings of the Institution of Civil Engineers, London, Vol.49, August, pp. 417-430.
14. Ghosh, S. N., and Kar, S. K. (1975) ''River flood plain interaction and distribution of boundary shear stress in a meander channel with flood plain.'' Proc. Inst. of Civ. Engrs., London, 59(2), 805–811.
15. Ghosh, S. N., and Roy, N. (1970). "Boundary shear distribution in open-channel flow." *J. Hydraul. Div., Am. Soc. Civ. Eng.,*96(4), 967–994.

16. Guo, J., and Julien, P. Y. (2005). ‘‘Boundary shear stress in smooth rectangular open channels.’’ Proc., 13th Int. Association of Hydraulic Research, APD Congress, Singapore, Vol. 1, 76–86.
17. Inglis, C.C.(1947). “Meander and Their Bering on River Training.” *Proceedings of the Institution of Civil Engineers, Maritime and Waterways Engineering Div., Meeting, 1947.*
18. Javid,S., and Mohammadi,M.(2012). ‘‘Boundary Shear Stress in a Trapezoidal Channel.” IJE TRANSACTIONS A: Basics Vol. 25, No. 4, (October 2012) 365-373.
19. Jia, Y., Blanckaert, K. & Wang, S.S. (2001). “Numerical simulation of secondary currents in curved channels.” Proc. 8th FMTM-congress, Tokyo.
20. Jing, H., Guo, Y., Li, C., & Zhang, J. (2009). “Three dimensional numerical simulation of compound meandering open channel flow by the Reynolds stress model.” *International Journal for Numerical Methods in Fluids*, 59, 927-943.
21. Kartha, V. C., and Leutheusser, H. J. (1970). “Distribution of tractive force in open-channels.” *J. Hydraul. Div., Am. Soc. Civ. Eng.,* 96(7), 1469–1483.
22. Kang H, Choi SU. (2006) “Reynolds stress modeling of rectangular open-channel flow.” *International Journal for Numerical Methods in Fluids 2006;* 51:1319 – 1334.
23. Khatua, K. K. (2008) “Interaction of flow and estimation of discharge in two stage meandering compound channels”. Thesis Presented to the National Institute of Technology, Rourkela, in partial fulfillments of the requirements for the Degree of Doctor of philosophy.

24. Khatua, K.K and Patra, K.C,(2010). Evaluation of boundary shear distribution in a meandering channel. Proceedings of ninth International Conference on Hydro-Science and Engineering, IIT Madras, Chennai, India, ICHE 2010, 74.
25. Knight, D. W. (1981). "Boundary shear in smooth and rough channels." *J. Hydraul. Div., Am. Soc. Civ. Eng.,* 107(7), 839–851.
26. Knight, D.W., and Demetriou, J.D., (1983), "Flood Plain and Main Channel Flow Interaction". *Journal of Hyd. Engg., ASCE* Vo.109, No.8, pp-1073-1092.
27. Knight, D.W., Demetriou, J.D. and Hamed, ME. (1984) "Boundary shears in smooth rectangular channels" *Journal of Hydr. Engin. ASCE* 110, pg.405-422.
28. Knight, D. W., and MacDonald, J. A. (1979). "Open-channel flow with varying bed roughness." *J. Hydraul. Div., Am. Soc. Civ. Eng.,* 105(9), 1167–1183.
29. Knight, D.W. and Patel, H.S., (1985), "Boundary shear in smooth rectangular ducts". *Journal of Hydraulic Engineering, ASCE,* Vol. 111, No. 1, 29-47.
30. Knight,D.W.,Yuan,Y.M.,and Fares,Y.R..(1992). "Boundary shear in meandering channels." *Proceedings of the Institution Symposium on Hydraulic research in nature and laboratory,* Wuhan, China (1992) Paper No.11017, Vol. 118, Sept., pp. 151-159.
31. Knight,D.W., and Sterling,M.(2000). '' Boundary shear in circular pipes running partially full." *Journal of Hyd. Engg., ASCE* Vol.126, No.4.
32. Lashkar A.B and Fathi M.M, (2010). "Wall and Bed Shear Forces in Open Channels."Research Journal of Physics, 4,1-10.

33. Launder BE, Spalding DB.(1974). "The numerical computation of turbulent flows." Computer Methods in *Applied Mechanics and Engineering 1974; 3:269 – 289.*
34. Leighly, J. B. (1932). "Toward a theory of the morphologic significance of turbulence in the flow of water in streams." Univ. of Calif. Publ. Geography,6(1), 1–22.
35. Lundgren, H., and Jonsson, I. G. (1964). "Shear and velocity distribution in shallow channels." *J. Hydraul. Div., Am. Soc. Civ. Eng.,*90(1),1–21.
36. Mellor GL, Herring HJ. "A survey of mean turbulent field closure." AIAA Journal 1973; 11:590 – 599.
37. Mohanty, P.K., Dash,S.S. and Khatua,K.K. (2012). "Flow Investigations in a Wide Meandering Compound Channel." International Journal of Hydraulic Engineering 2012, 1(6) : 83-94
38. Myers,W.R.C., and Elsawy (1975). "Boundary Shear in Channel with Floodplain." *Journal of Hydraulic Engineering, ASCE*, Vol.101, HY7, pp. 933-946.
39. Myers, W. R. C. (1978). "Momentum transfer in a compound channel." *J. Hydraul. Res.,16(2),* 139–150.
40. Patra, K.C, and Kar, S. K. (2000), "Flow Interaction of Meandering River with Floodplains". *Journal of Hydr. Engrg., ASCE,* 126(8), 593–604.
41. Patra, K.C., and Kar, S.K., Bhattacharya.A.K. (2004). "Flow and Velocity Distribution in Meandering Compound Channels." *Journal of Hydraulic Engineering*, *ASCE*, Vol. 130, No. 5. 398-411.

42. Rajaratnam, N., and Ahmadi, R.M. (1979). "Interaction between Main Channel and Flood Plain Flows." *Journal of Hydraulic Division*, *ASCE,* Vol..105, No. HY5, pp. 573-588.
43. Rameshwaran P, Naden PS.(2003) "Three-dimensional numerical simulation of compound channel flows." *Journal of Hydraulic Engineering (ASCE) 2003;* 129:645 – 652.
44. Rhodes, D. G., and Knight, D. W. (1994). ''Distribution of Shear Force on Boundary of Smooth Rectangular Duct.'' *Journal of Hydralic Engg.*, 120-7, 787– 807.
45. Salvetti MV, Zang Y, Street RL and Banerjee S. (1997). "Large-eddy simulation of free surface decaying turbulence with dynamic subgrid -scale models." Physics of Fluids. 9, pp. 2405.
46. Shiono, K., Muto, Y., Knight, D.W. & Hyde, A.F.L.(1999). "Energy Losses due to Secondary Flow and Turbulence in Meandering Channels with Overbank Flow." *Journal of Hydraulic Research*, IAHR, Vol. 37, No. 5, pp. 641-664.
47. Speziale CG, Sarkar S, Gatski T. (1991). "Modeling the pressure strain correlation of turbulence: an invariant dynamical systems approach." *Journal of Fluid Mechanics* 1991; 227:245 – 272.
48. Sugiyama H, Hitomi D, Saito T. (2006). "Numerical analysis of turbulent structure in compound meandering open channel by algebraic Reynolds stress model." *International Journal for Numerical Methods in Fluids* 2006; 51:791 – 818.
49. Thomas TG. and Williams J.(1995a). "Large eddy simulation of a symmetric trapezoidal channel at Reynolds number of 430,000." *J. Hydraul. Res.*. 33(6), pp. 825-842.

50. Thomas TG. and Williams J.(1995b). "Large eddy simulation of turbulent flow in an asymmetric compound open channel." *J. Hydraul. Res.* 33(1), pp. 27-41.
51. Thomas TG. and Williams J.(1999). Large eddy simulation of flow in a rectangular open channel. *J. Hydraul Res.* 37(3), pp. 345-361.
52. Toebes, G.H., and Sooky, A.A.(1967). "Hydraulics of Meandering Rivers with Floodplains." *Journal of the waterways and Harbor Division, Proceedings of ASCE*, Vol.93, No.WW2, May, pp. 213-236.
53. Wormleaton, P.R., Allen, J.,and Hadjipanos, P.(1982). "Discharge Assessment in Compound Channel Flow." *Journal of Hydraulic Engineering, ASCE*, Vol.108, No.HY9, pp. 975-994.
54. Yang, S. Q., and Lim, S. Y. (1997). "Mechanism of energy transportation and turbulent flow in a 3D channel." *J. Hydraul. Eng.,* 123(8), 684–692.
55. Yang, S. Q. and Mc Corquodale, John A. (2004) "Determination of Boundary Shear Stress and Reynolds Shear Stress in Smooth Rectangular Channel Flows." *Journal of Hydr. Engrg.,* Volume 130, Issue 5, pp. 458-462.
56. Zheleznyakov, G.V.(1965). "Interaction of Channel and Floodplain Streams." *Proc. 14th Congress of IAHR,* 5, Paris, France, pp. 144-148.

## Publications from the Work

### A: Published

1. Patnaik, M., Patra.K.C., Khatua, K.K., Mohanty, L. (2012) "Boundary Shear Distribution in Highly Sinuous Meandering Channels" Proceedings of National Conference on Hydraulic and Water Resources, IIT Bombay, India, HYDRO 2012, 1233-1242.
2. Mohanty, L., Patra.K.C., Khatua, K.K., Patnaik, M. (2012) "Depth-Averaged Velocity Distribution in Trapezoidal Meandering Channels" Proceedings of National Conference on Hydraulic and Water Resources, IIT Bombay, India, HYDRO 2012, 625-634.
3. Patnaik, M., Mohanty, L., Patra.K.C. (2013) "Wall and Bed Shear Distribution in Meandering Channels" Symposium on Sustainable Infrastructure Development, IIT, Bhubaneswar, Odisha, India, IWMSID 2013, 374-382.
4. Mohanty, L., Patnaik, M., Patra.K.C. (2013) "Lateral Distribution of Depth-Averaged Velocity in Trapezoidal Meandering Channels" Symposium on Sustainable Infrastructure Development, IIT, Bhubaneswar, Odisha, India, IWMSID 2013, 383-389.

**5. B: Accepted for Publication**

1. Patnaik, M., Patra.K.C., Khatua, K.K., Mohanty, L. (2012) "Modeling Boundary Shear Stress in Highly Sinuous Meandering Channels" accepted for ISH *Journal of Hydraulic Engineering,* Taylor & Francis Group, UK.
2. Mohanty, L., Patra.K.C., Khatua, K.K., Patnaik, M. (2012) "Modeling Depth-Averaged Velocity in Trapezoidal Meandering Channels" accepted for ISH *Journal of Hydraulic Engineering,* Taylor & Francis Group, UK.